



RESEARCH ARTICLE

Synthesis of Novel 1,3,5-Triazine Analogues With Selective Activity Against Pancreatic (Capan-1) and Colorectal (HCT-116) Carcinomas: Anticancer Potential and DNA-Binding Affinity

Shazia Asghar¹ | Aftab Aziz¹ | Shahid Hameed¹  | Bahjat A. Saeed² | Risala H. Allami³ | Najim A. Al-Masoudi⁴ 

¹Department of Chemistry, Quaid-I-Azam University, Islamabad, Pakistan | ²Department of Chemistry, College of Education for Pure Science, University of Basrah, Basrah, Iraq | ³Department of Molecular and Medical biotechnology, College of Biotechnology, Al-Nahrain University, Baghdad, Iraq | ⁴Department of Chemistry, College of Science, University of Basrah, Basrah, Iraq

Correspondence: Shahid Hameed (shameed@qau.edu.pk) | Najim A. Al-Masoudi (najim.al-masoudi@gmx.de)

Received: 21 April 2025 | **Revised:** 1 July 2025 | **Accepted:** 14 July 2025

Keywords: anticancer activity | DNA-binding potential | molecular docking study | molecular dynamics simulation | s-triazine derivatives

ABSTRACT

A series of 2-(2-arylidenhydrazinyl)-4,6-bis(substituted-phenoxy)-1,3,5-triazines (compounds **3a–o** to **7a–o**) was synthesized and evaluated for DNA-binding affinity using calf thymus DNA. Based on their DNA interaction profiles, the top three compounds from each series were selected for in vitro anticancer screening against eight human cancer cell lines, encompassing both solid tumors (glioblastoma, pancreatic adenocarcinoma, colorectal carcinoma, and lung carcinoma) and hematological malignancies (acute lymphoblastic leukemia, acute myeloid leukemia, chronic myeloid leukemia, and non-Hodgkin lymphoma). Among the tested compounds, **5i** and **7b** demonstrated the highest anticancer potency against pancreatic adenocarcinoma (Capan-1), with IC₅₀ values of 2.4 and 1.9 μM, respectively. Notably, compound **5i** also exhibited strong cytotoxicity against colorectal carcinoma (HCT-116), with an IC₅₀ of 2.2 μM. Additional analogues namely **3i**, **3l**, **6g**, **6l**, and **7m** displayed IC₅₀ values ranging from 7.4 to 42.2 μM across the panel of cancer cell lines, highlighting the superior activity of **5i** and **7b** as promising antiproliferative agents. Molecular docking studies revealed that compound **7b** formed strong interactions with the prenyl-binding protein PDEδ, and subsequent molecular dynamics simulations confirmed the stability of the **7b**–PDEδ complex, supporting its potential as a targeted anticancer agent.

1 | Introduction

1,3,5-Triazine derivatives have garnered considerable attention from medicinal chemists due to their exceptional pharmacological properties [1]. These compounds have shown a wide range of applications and significant biological potential, including antimicrobial [2, 3], anticancer [4–11], antiviral [12], antiplasmodial, herbicidal [13], antimalarial [14], antifungal [15], anti-inflammatory [16], antidiabetic [17], and cystic fibrosis transmem-

brane conductance regulator (CFTR) modulatory effects [18]. Literature revealed that exchange of different functional groups on 1,3,5-triazine nucleus displayed distinct effects on malignant cell proliferation [19]. Several 2,4,6-trisubstituted 1,3,5-triazine derivatives have demonstrated notable antitumor activities [20] and have served as scaffolds for the development of various clinically approved drugs and drug candidates. For instance, tretamine (**1**, Figure 1) [21] is utilized in chemotherapy, while hexamethylmelamine (altretamine (**2**, Figure 1); HMM) and its

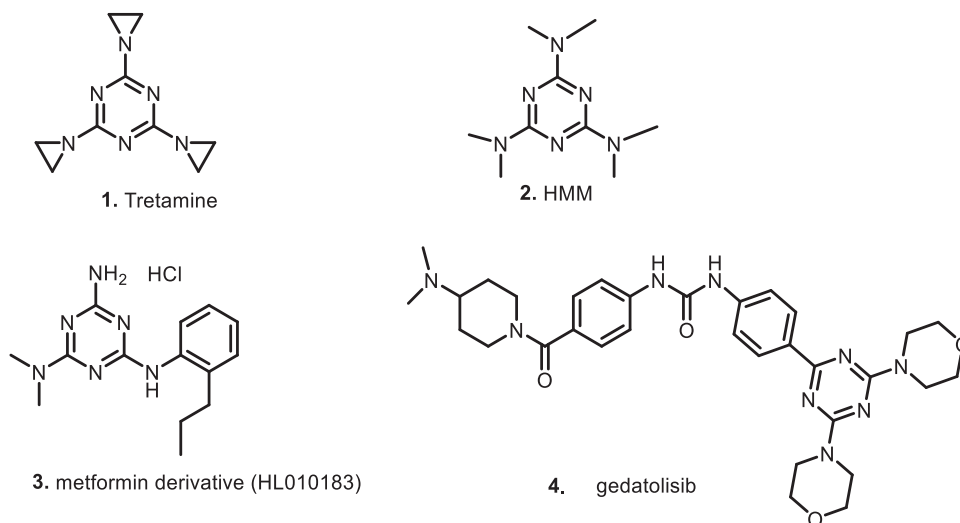


FIGURE 1 | Some biologically active substituted 1,3,5-triazine compounds.

hydroxylated analogue are used in the treatment of epithelial ovarian carcinoma [22]. A recently developed metformin derivative (**3**, Figure 1) has shown potential in inhibiting the growth and metastasis of triple-negative breast cancer cells [23]. In addition, gedatolisib (**4**, Figure 1) [24] and altretamine [25, 26] are alkylating antineoplastic agents employed in the treatment of breast and ovarian cancers, respectively.

Compounds containing an imine or azomethine ($-\text{C}=\text{N}-$) functional group have been proven to be versatile pharmacophores in the design and development of various bioactive lead compounds [27]. Recently, a series of *s*-triazine-hydroxybenzylidene hydrazone derivatives has been reported as dual-effective inhibitors against both wild-type (WT) and mutant epidermal growth factor receptor tyrosine kinase inhibitors (EGFR TKIs) [28]. Al-Rasheed et al. [29, 30] explored a series of *s*-triazine hydrazone analogues for in vitro anticancer activity. Among these compounds, 4,4'-(6-(2-(pyridin-2-ylmethylene)hydrazinyl)-1,3,5-triazine-2,4-diyl)dimorpholine demonstrated notable anticancer efficacy, with half-maximal inhibitory concentration (IC_{50}) values of 1.0 and 0.98 μM against MCF-7 and HCT-116 cell lines, respectively. The study also highlighted that the activity is significantly affected by the nature of the substituents on both the *s*-triazine and benzylidene moieties. Furthermore, Cetin et al. [31] reported the synthesis of 1,2,4-triazine derivatives bearing sulfonamide hybrids and evaluated their effects on AChE and GST enzymes under both in silico and in vitro conditions. Albericio et al. [32] recently introduced a novel series of *s*-triazine Schiff base derivatives and reported their preliminary antiproliferative activities. In addition, a series of *s*-triazine hydrazone derivatives was evaluated for their potential as selective dual inhibitors of PI3K α and mTOR. Among these, 5-(4-(5-((4-(methylsulfonyl)piperazin-1-yl)methyl)thiophene-2-yl)-6-morpholino-1,3,5-triazin-2-yl)pyrimidine-2-amine emerged as a promising lead compound, exhibiting strong inhibitory activity with IC_{50} values of 7.0 nM for PI3K α and 48 nM for mTOR. Moreover, a new series of disulfide-1,2,4-triazine derivatives was efficiently synthesized by Cetin et al. [33] and showed significant inhibitory activity against both AChE and GST.

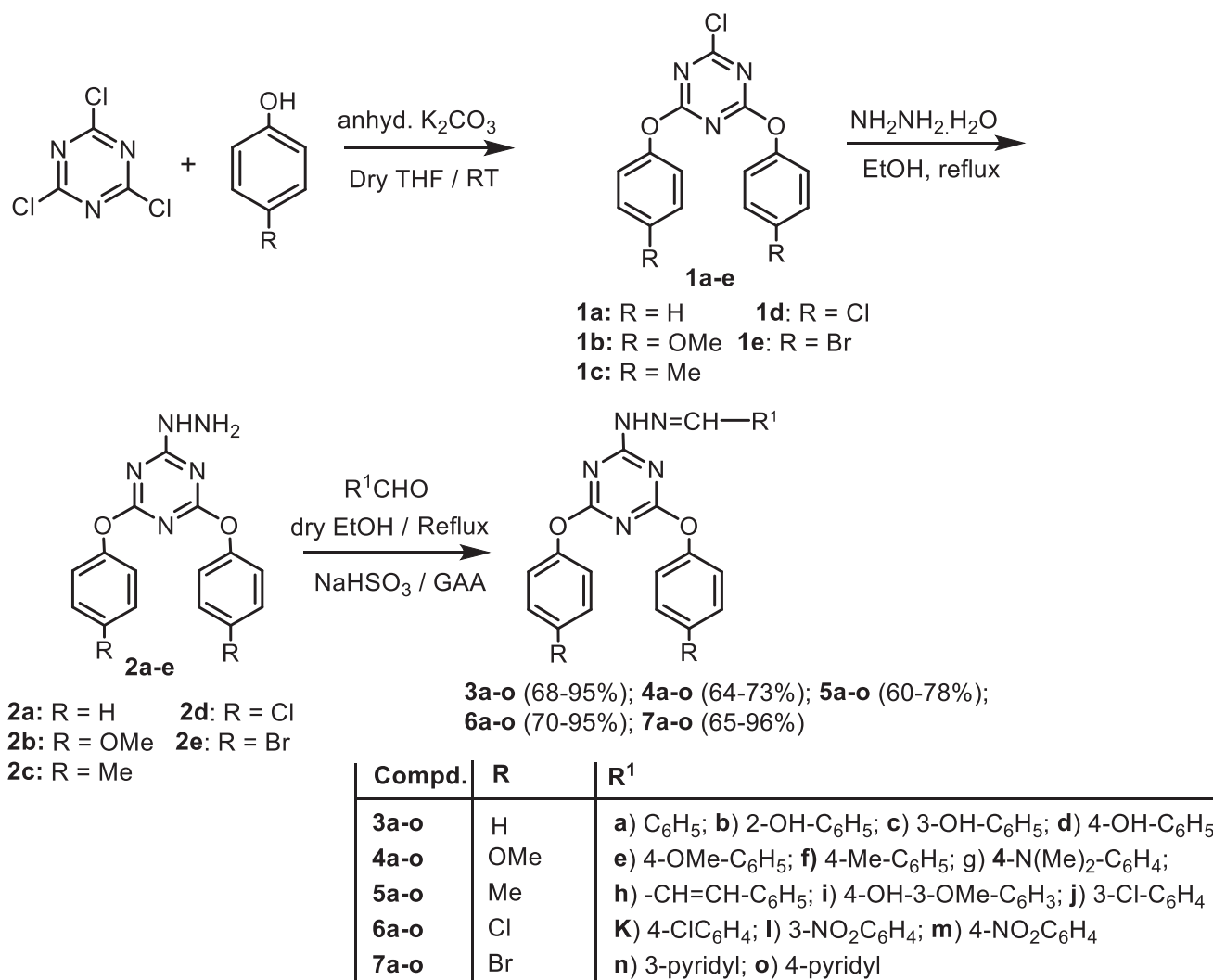
Considering the diverse pharmacological properties of *s*-1,3,5-triazine derivatives and analogues, and building on our previous research on triazine analogues with anticancer activity [34], we now present novel *s*-1,3,5-triazine hydrazone derivatives conjugated with 4,6-bis(substituted-phenoxy) groups, and evaluation of their DNA-binding interactions and anticancer activity.

2 | Results and Discussion

2.1 | Chemistry

Synthesis of 2-(2-arylidenehydrazinyl)-4,6-bis(substituted-phenoxy)-1,3,5-triazines **3a–o** to **7a–o** was achieved in a multistep sequence using readily available starting materials [35] (Scheme 1). In the first step, cyanuric chloride and five differently substituted phenols were reacted to synthesize 2-chloro-4,6-bis(substituted-phenoxy)-1,3,5-triazines **1a–e**, which were further treated with hydrazine monohydrate to obtain 2-hydrazino-4,6-bis(substituted-phenoxy)-1,3,5-triazine derivatives **2a–e**. Treatment of **2a–e** with substituted benzaldehydes in the presence of catalytic amounts of NaHSO_3 /glacial HOAc afforded the target analogues **3a–o** to **7a–o**. All of the newly synthesized compounds were obtained in excellent yields and purities. The characterization of the synthesized compounds was carried out using spectral analysis.

The structures of compounds **3a–o** to **7a–o** were confirmed using IR, NMR, and high-resolution mass spectrometry. Evidence of successful synthesis was supported by IR spectra, which showed characteristic absorption bands in the range of $3311\text{--}3223\text{ cm}^{-1}$, corresponding to the N–H stretching vibrations of the hydrazinyl group. The absence of peaks corresponding to the primary amine group further confirmed the formation of the hydrazone linkage. The ^1H NMR spectra were marked by the presence of imine protons appearing as singlets in the range of δ 12.17–8.56 ppm. The formation of the azomethine linkage was further supported by sharp singlets observed between δ 8.32 and 7.71 ppm, corresponding to the imine protons. In the ^{13}C NMR spectra, signals observed in the range of δ 147.2 to 141.1 ppm were assigned to



SCHEME 1 | Synthesis of 2-(2-arylidenehydrazinyl)-4,6-diaryloxy-1,3,5-triazines (3a-o to 7a-o).

the azomethine carbons (C-7). Additional signals corresponding to the newly introduced benzaldehyde ring appeared in the aromatic region of the ¹³C NMR spectra, ranging from δ 161.2 to 108.6 ppm (Supporting Information). The other aromatic and aliphatic carbon atoms were resonating in the expected region (cf. Section 5). The high-resolution mass spectra (HRMS) (ESI) spectra confirmed the molecular mass of the synthesized compounds.

2.2 | DNA-Binding Studies

Agents that induce DNA damage led to changes in the fundamental structure of DNA, that is why they have been widely used in cancer chemotherapy. Even today, cancer treatment remains heavily dependent on chemotherapeutic drugs. Focusing on DNA as a central target for antineoplastic therapies has led to the development of several new anticancer drugs, including cisplatin, carboplatin, 5-fluorouracil, oxaliplatin, picoplatin, doxorubicin, and daunorubicin [36]. However, the enhanced DNA repair capacity in tumor cells often leads to the failure of many of these drugs [37, 38]. Consequently, identifying new molecules as therapeutic targets, understanding the signaling pathways

associated with DNA damage, and gaining insight into DNA-drug interactions are essential for comprehending their mechanisms of action [39]. UV-visible absorption spectroscopy is the most widely used techniques for studying DNA stability and the interactions between DNA and drug molecules. While other methods are also employed, UV-visible spectroscopy remains the preferred choice for such studies [40]. By maintaining a constant DNA concentration and varying the drug dilution, or vice versa, shifts in UV absorption can be measured. Interactions between DNA and drug molecules often lead to spectral changes, such as hyperchromism, hypochromism, bathochromic shifts, or hypsochromic shifts in the DNA absorption spectrum. These changes are analyzed to determine the binding affinity between the DNA duplex and the ligand molecules, offering valuable insights into the nature and strength of their interactions [41].

All the synthesized compounds, **3a-o** to **7a-o**, were evaluated for their DNA-binding potential using UV-visible spectroscopy. The interaction was studied by observing shifts in the UV absorption of calf thymus DNA (ct-DNA) while keeping the drug concentration constant and varying the ct-DNA dilutions. A notable increase in absorption maxima, accompanied by a minimal bathochromic (red) shift, was observed for derivatives **3a-o** and

their DNA adducts. This phenomenon may be attributed to DNA denaturation upon interaction with the test compounds. All compounds in the **3a–o** series exhibited hyperchromism, indicating electrostatic interactions between the test compounds and the DNA nucleotides. The electrostatic interaction mechanism, resulting from the binding of the compounds to the DNA phosphate groups, is well-supported by prior research [42]. In addition, the observed uncoiling of DNA and the increase in absorbance maxima in the presence of free bases are consistent with findings previously reported in the literature [43].

Among the derivatives **4a–o**, compound **4o**, which contains a 4-pyridyl group and methoxy-substituted bisphenols, showed the strongest interactions with DNA, with its absorption maxima more than doubling. Similarly, compounds **4c** and **4l** showed relatively stronger interactions with DNA. The pronounced hyperchromism observed may be attributed to π - π stacking interactions between the aromatic and heteroaromatic rings. A significant increase in absorption maxima was observed for the DNA complexes of compounds **5a–o**, likely due to DNA denaturation upon interaction with the test compounds. Among these, derivatives **5e**, **5i**, and **5j** demonstrated the most pronounced DNA interactions. In addition, all compounds in the **6a–o** series exhibited a hyperchromic effect, with some showing a slight bathochromic shift of 3–5 nm. Among these, compounds **6c** and **6g** displayed the strongest DNA-binding affinity, as evidenced by notable increases in their absorption maxima. Similarly, within the **7a–o** series, compound **7b** exhibited a strong interaction with DNA, characterized by a decrease in absorption maxima, a bathochromic shift, and the emergence of new spectral peaks, all indicative of robust binding. DNA denaturation is suggested to occur through a combination of electrostatic binding and intercalation. Furthermore, compounds **7i**, **7j**, **7m**, and **7o** demonstrated significant DNA-binding interactions, as indicated by hyperchromism and a slight bathochromic shift of 3–5 nm. The binding constants for most of the compounds were similar to those of commercially available intercalators and electrostatic or groove binders. High Gibbs free energy values suggested that the interactions between the compounds and DNA were spontaneous, resulting in the formation of stable complexes. These interactions were analyzed using UV–visible absorption spectra, with binding constants graphically interpreted (Figure 2). Compounds **3i**, **3l**, **3n**, **4c**, **4l**, **4o**, **5e**, **5i**, **5j**, **6c**, **6g**, **6l**, **7b**, **7m**, and **7o**, which showed relatively stronger DNA-binding interactions, were selected for further evaluation of in vitro anticancer activity against a panel of eight human cancer cell lines, representing both solid and hematological tumors, using MTS assay [44].

2.3 | In Vitro Anticancer Assay

The cytotoxic potential of selected newly synthesized compounds was assessed in vitro against a panel of human tumor cell lines using MTS assay [44]. The panel included Capan-1 (pancreatic adenocarcinoma), HCT-116 (colorectal carcinoma), LN-229 (glioblastoma), NCI-H460 (lung carcinoma), DND-41 (acute lymphoblastic leukemia), HL-60 (acute myeloid leukemia), K-562 (chronic myeloid leukemia), and Z-138 (non-Hodgkin lymphoma). Etoposide (ETP) was used as the reference drug. The results, presented in Table 1, demonstrated that compounds with a 1,3,5-triazine scaffold substituted with bis-arylether moi-

eties exhibited notable cytotoxic activity. Compounds **5i** and **7b** exhibited significant cytotoxic activity against pancreatic adenocarcinoma cell line Capan-1 with IC₅₀ values of 2.4 and 1.9 μ M, respectively. In contrast, the analogues **3i**, **3l**, **6g**, **6l**, and **7m** showed IC₅₀ values ranging from 7.4 to 42.2 μ M across the entire panel of cell lines, while other compounds displayed IC₅₀ values of > 100 μ M. In addition, compound **5i** demonstrated IC₅₀ values ranging from 2.2 to 22.7 μ M across the other cell lines. However, all compounds displayed IC₅₀ values ranging from 5.2 to 80.5 μ M against LN229 cell line, except the analogues **4l**, **4o**, and **7o** which have IC₅₀ values of > 100 μ M. Furthermore, compound **7b** had noteworthy antiproliferative activity with IC₅₀ values of 10.4, 14.5, 7.1, and 10.2 μ M against HCT-116, DND-41, HL-60, and Z-138 cell lines, respectively.

In their SAR study, Guenin et al. [45] have reported that halogen substituents and their positions on the phenyl group play a critical role in influencing the inhibition of tumor cell proliferation in vitro. They found that the presence of a *para*-bromo substituent on the phenyl ring significantly enhances the anticancer activity of 1-hydroxymethylene-1,1-bisphosphonic acids (HMBP). Our current findings, along with our previous results [34], align with the results of Guenin et al. Compounds **7b** featuring a *para*-bromo substituent on the phenyl ring, demonstrated superior antiproliferative activity (IC₅₀ = 1.9 μ M) compared to other groups (OMe, Me, Cl). The observations suggest that the inhibitory potential of triazine analogues is significantly influenced by the substitution patterns on the diphenoxy rings attached to the C-3 and C-4 positions of 1,2,3-triazine backbone, as well as by the substituents on the phenyl ring of the imine group at C-2 position. These findings underscore the importance of synthesizing various substituted 1,3,5-triazine derivatives to enhance antiproliferative activity against diverse cancer cell lines. Consequently, triazine hybrids represent promising scaffolds for the development of novel anticancer therapies. Recently, Dong et al. [46] provided an extensive review of the anticancer activity of 1,2,3-, 1,2,4-, and 1,3,5-triazine hybrids, detailing their structure–activity relationships and mechanisms of action from 2017 to the present.

3 | Molecular Docking Study

Molecular docking study is a computational technique that predicts the binding affinity of ligands to receptor proteins. Although it has potential uses in nutraceutical research, it has developed into a formidable tool for drug development [47]. In this study, the AutoDock4 [48] was employed for docking calculations, and the obtained docking results were visualized and analyzed using MGLTools. The receptor molecule was prepared by elimination of water molecules from their structures and then subjected to correction and three-dimensional (3D) protonation refinement.

The KRAS oncogene product is widely recognized as a critical target in anticancer drug development [49]. Zimmermann et al. [50] emphasized the significance of proper localization and signaling of farnesylated KRAS, a process regulated by the prenyl-binding protein phosphodiesterase delta (PDE δ). This interaction plays a crucial role in maintaining the spatial organization of KRAS by promoting its cytoplasmic diffusion. Mutations in the KRAS gene are a major driver of pancreatic cancer progression. The study emphasized that small molecules

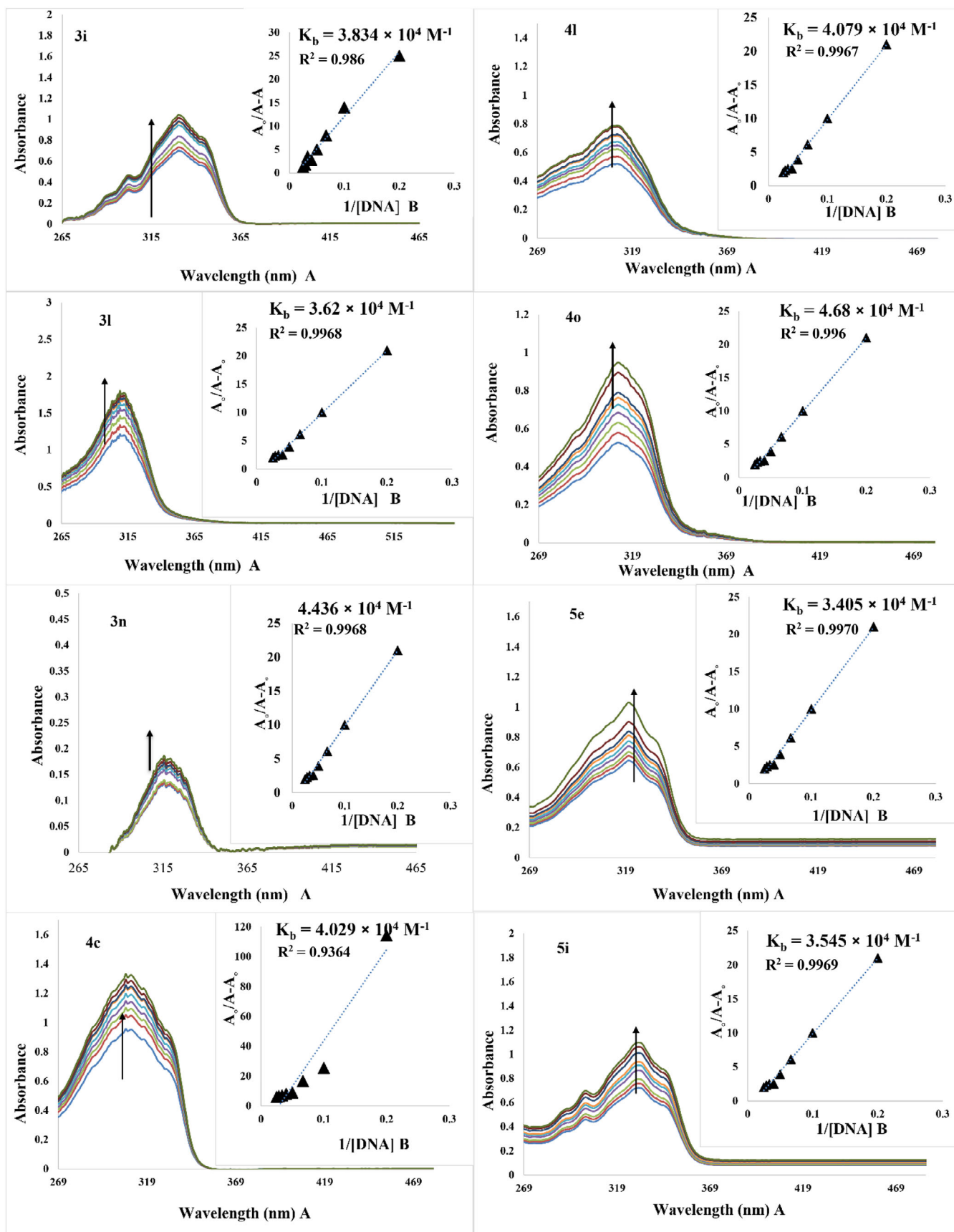


FIGURE 2 | (A) UV-visible spectra of compounds 3i, 3l, 3n, 4c, 4l, 4o, 5e, 5i, 5j, 6c, 6g, 6l, 7b, 7m, and 7o in the absence and presence of DNA (5–40 μ M). (B) Graph between $1/[DNA]$ and $A_0/A - A_0$ for calculation of binding constant for 3i, 3l, 3n, 4c, 4l, 4o, 5e, 5i, 5j, 6c, 6g, 6l, 7b, 7m, and 7o.

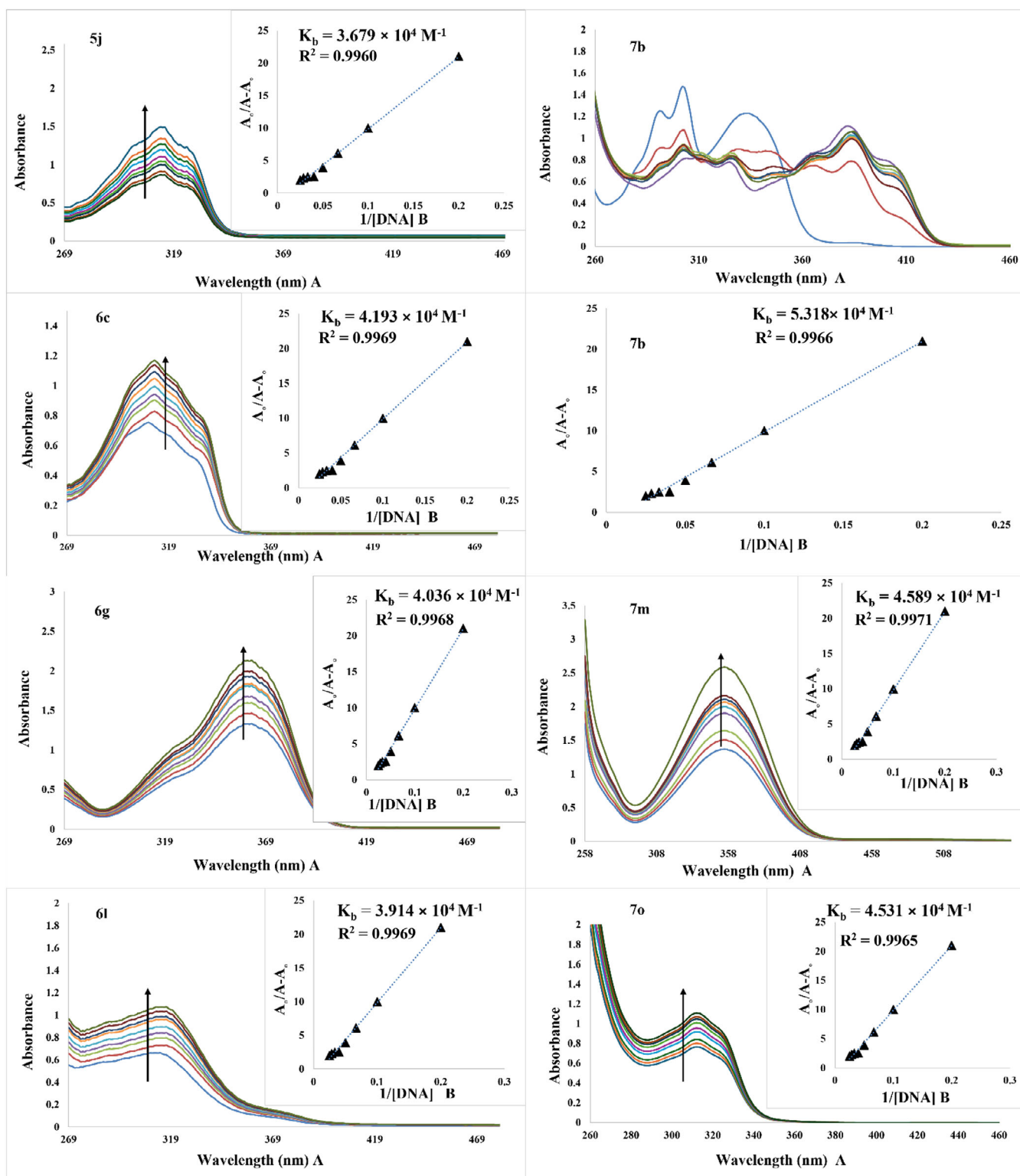


FIGURE 2 | (Continued)

disrupting the KRAS–PDE δ interaction offer a novel approach to interfere with KRAS localization and downstream signaling, presenting a promising avenue for developing new anticancer therapies. Furthermore, Luo [51] reviewed the functional implications of mutant KRAS in pancreatic cancer and discussed emerging therapeutic strategies targeting this oncogenic pathway. Collectively, these findings underscore the KRAS–

PDE δ interaction as an attractive target for inhibiting the oncogenic activity of mutant KRAS, potentially guiding future drug discovery efforts focused on RAS-driven cancers.

To identify a potential anticancer lead compound, we selected compound **7b** for molecular docking studies, as it exhibited the lowest IC₅₀ value among the 1,3,5-triazine derivatives. Docking

TABLE 1 | In vitro anticancer activity against a broad panel of cancer cell lines.

Comp.	IC ₅₀ (μM)							
	Cell lines							
	Capan-1	HCT-116	LN-229	NCI-H460	DND-41	HL-60	K-562	Z-138
3i	7.4	42.1	39.00	14.0	14.4	10.4	17.2	9.5
3l	42.2	> 100	25.4	> 100	> 100	> 100	93.3	> 100
3n	> 100	> 100	9.5	> 100	> 100	> 100	> 100	> 100
4c	> 100	> 100	80.5	> 100	> 100	> 100	> 100	> 100
4l	> 100	> 100	> 100	> 100	> 100	> 100	> 100	> 100
4o	> 100	> 100	> 100	> 100	> 100	> 100	> 100	> 100
5c	> 100	> 100	14.9	> 100	> 100	11.9	> 100	> 100
5i	2.4	2.2	9.6	10.7	8.5	11.8	8.5	22.7
6c	> 100	> 100	41.1	> 100	> 100	> 100	> 100	> 100
6g	19.4	45.4	8.2	14.2	43.6	53.6	7.4	26.9
6l	33.4	54.6	5.2	38.4	13.5	15.9	28.5	11.4
7b	1.9	10.4	13.1	> 100	14.5	7.1	> 100	10.2
7m	8.5	> 100	21.7	> 100	42.9	17.8	38.9	13.4
7o	> 100	> 100	> 100	> 100	> 100	> 100	> 100	> 100
ETP	0.45	1.02	2.40	3.65	2.80	0.40	1.44	0.60

Abbreviation: ETP, etoposide.

was performed using AutoDock4 with the 3D crystal structures of the PDEδ prenyl-binding pocket in pancreatic ductal adenocarcinoma (PDB IDs: 5X74, 4JV6, and 5E80) [52]. Compound **7b** was assessed based on the binding energies of its top conformations, yielding scores of −10.2, −9.5, and −11.7 kcal/mol, respectively. These results suggest a strong and selective affinity of compound **7b** for the active sites of the targeted protein structures.

Figure 3A shows the docking results, depicting the precise orientation of compound **7b** within the binding site of the cell cycle-related protein PDEδ (PDB: 4X74). The analysis revealed two hydrogen bonds: one between the N-5 atom of the triazine core and Arg61 (2.228 Å), and another between the N-1 atom of the same ring and Gln78 (2.210 Å). In addition, several nonbonded residues: Trp90, Phe91, Ile109, Glu89, Leu147, Ala111, and Pro113 were located near compound **7b**, indicating potential stabilizing interactions within the binding pocket.

Figure 3B presents the docking analysis of compound **7b** with the protein PDEδ (PDB: 5JVB), revealing a hydrogen bond (1.667 Å) between the N-5 atom of the triazine core and Arg61. In addition, several nonbonded amino acid residues: Trp90, Leu22, Ile129, Met20, Leu38, Ile109, Ile53, Try149, Leu54, and Glu88 were observed surrounding the compound, suggesting possible stabilizing interactions within the binding pocket.

Figure 3C illustrates that compound **7b** is well-positioned within the active site of the PDEδ protein. A hydrogen bond was observed between the N-5 atom of the triazine core and Arg61 (2.228 Å). In addition, several nonbonded amino acid residues: Trp90, Leu123, Tyr149, Leu54, Ile53, Ala111, Val59, Met20, Ile129, Val145, and Leu38 were found surrounding compound **7b**,

indicating potential stabilizing interactions within the binding pocket.

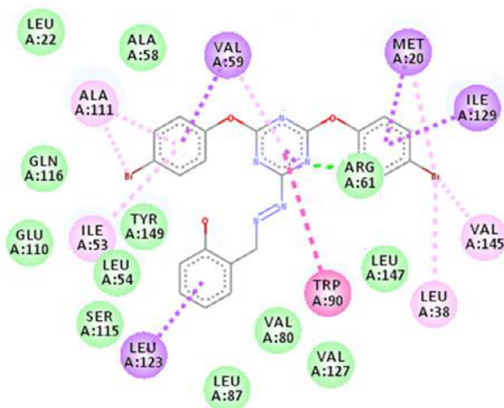
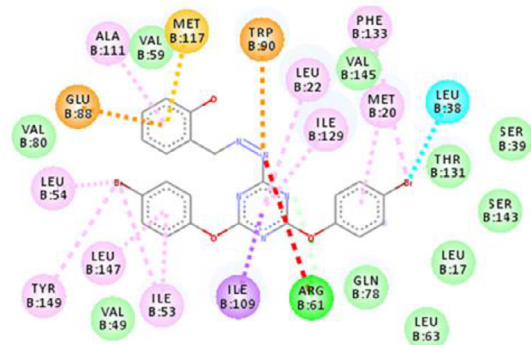
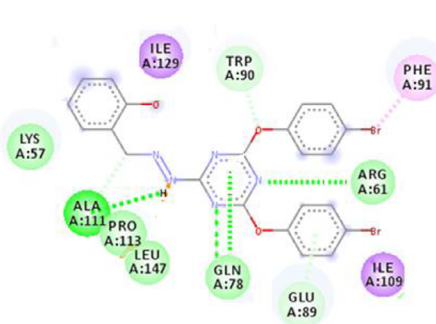
In summary, our structure-based optimization led to the identification of compound **7b** as a potent inhibitor of the KRAS–PDEδ interaction. Compound **7b** selectively targets the prenyl-binding pocket of PDEδ with micromolar affinity, primarily through a key interaction with Arg61. As a result, it effectively disrupts oncogenic RAS signaling and inhibits the in vitro proliferation of Capan-1 human pancreatic ductal adenocarcinoma cells, which are dependent on mutant KRAS. These results underscore the potential of **7b** as a lead compound and may inspire further drug discovery efforts aimed at targeting oncogenic RAS. Table 2 summarizes the binding energies, inhibition constants (K_i), and hydrogen bonding interactions (H.B.) of the triazine analogue **7b** with PDEδ.







4 | Molecular Dynamics Simulation






4.1 | Root Mean Squared Deviation

Molecular dynamics (MD) is a computer simulation technique used to study the behavior of biological molecules, such as proteins and nucleic acids, by visualizing the motion of atoms and molecules over time, enabling a deeper understanding of ligand–protein interactions and stability.

Compound **7b** exhibited high docking scores and maintained a stable conformation within the binding pocket, consistently remaining at a fixed distance from the protein’s center of mass throughout the simulation, as confirmed by the production run



-  van der Waals
-  Conventional Hydrogen Bond
-  Carbon Hydrogen Bond
-  Halogen (Cl, Br, I)
-  Unfavorable Positive-Positive
-  Pi-Cation

-  Pi-Anion
-  Pi-Sigma
-  Pi-Sulfur
-  Alkyl
-  Pi-Alkyl

8 of 23

TABLE 2 | Energies and inhibition constants (K_i) of the binding of the triazine analogue **7b** with protein PDE δ , hydrogen bonding (H.B.) and their lengths in Å.

Protein	Binding energy (kcal/mol)	K_i (nM)	Intramolecular energy	Internal energy	Torsional energy	Unbound extended energy	H.B.
5X74	-10.15	36.4	-11.33	-1.81	2.39	-0.61	N-5:Arg61 (2.228) N-1:Gln78 (2.210)
4JV6	-9.48	111.86	-10.66	-1.82	2.039	-0.61	N-1:Arg61 (1.667)
5E80	-11.69	2.72	-12.92	-1.76	2.39	-0.61	N-3:Arg61 (2.077)

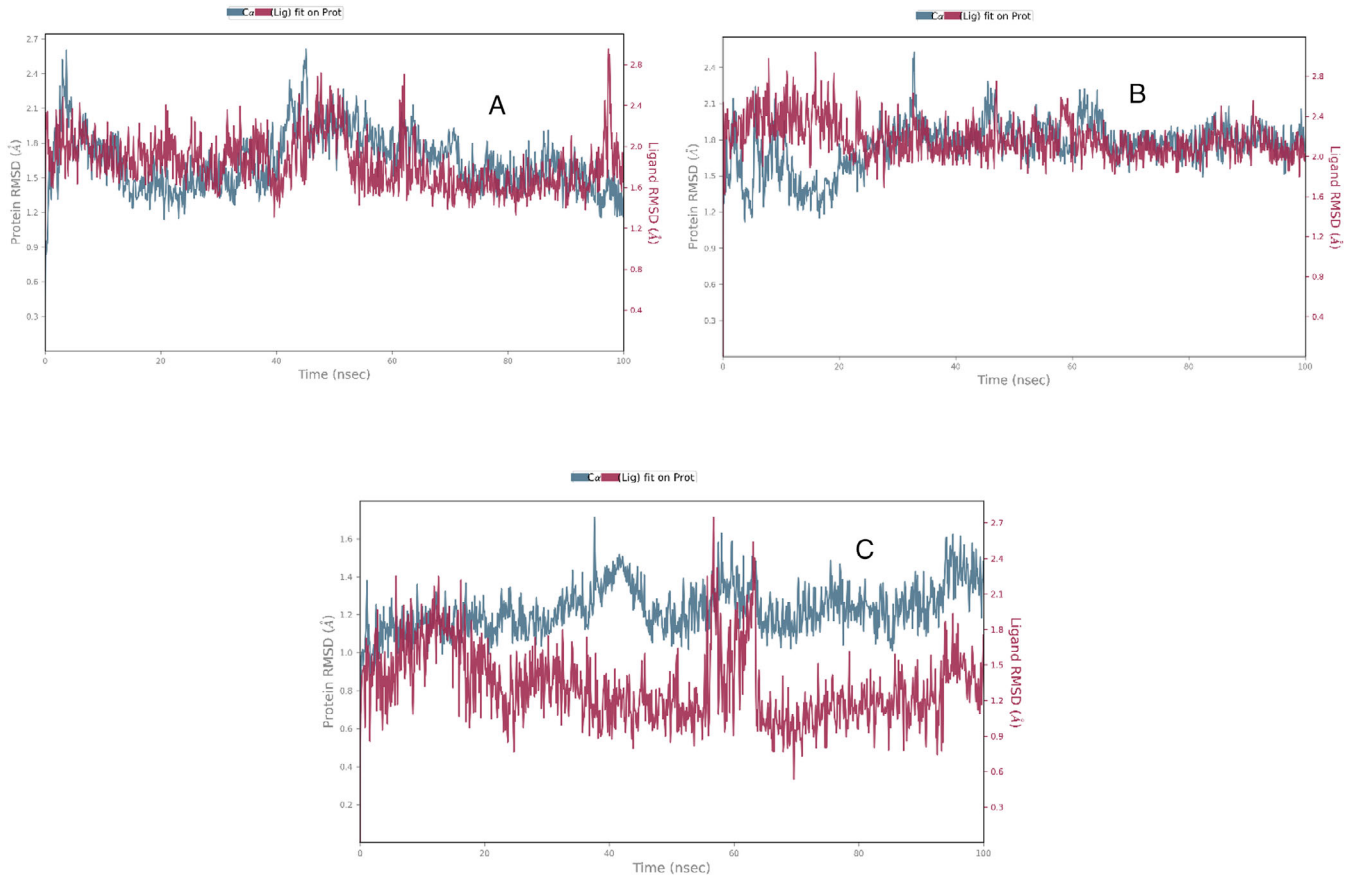


FIGURE 4 | RMSD Plot for compound **7b** with pdb structures (A) 5X74, (B) 4jvb, and (C) 5e80.

analyses. Therefore, we selected complex **7b** for an in-depth MD analysis with the retinal rod rhodopsin-sensitive cGMP 3',5'-cyclic PDE δ receptor, focusing on the 5X74, 4jvb, and 5e80 crystal structures. This calculation identified the number of active interactions between inhibitor **7b** and the residues within the active sites of the enzymes under study.

The average root mean squared deviation (RMSD) values for the **7b**_5X74, **7b**_4jvb, and **7b**_5e80 complexes were calculated to be 1.77, 1.89, and 1.36 Å, respectively. For the **7b**_5X74 complex, the average and maximum RMSDs were 1.8 and 2.3 Å, which were higher than those of the **7b**_4jvb complex (1.6 and 2.1 Å, respectively) as shown in Figure 4. Notably, the **7b**_5e80 complex exhibited relatively lower RMSD fluctuations compared to the other two complexes, indicating greater structural stability. Furthermore, the ligand RMSD for the **7b**_5e80 complex was found to

be 0.9 Å, suggesting a more stable interaction between compound **7b** and the PDE δ protein (PDB: 5e80) during the simulation. This stability correlates well with the low-binding energy observed in the docking studies, supporting the high-binding affinity of compound **7b** for the 5e80 target.

4.2 | Root Mean Square Fluctuation

Root mean square fluctuation (RMSF) is utilized to measure the fluctuation of individual amino acid residues during the complexation with compound **7b**. High RMSF values reflect the flexibility of amino acids, while low RMSF values signify the stability of specific amino acid regions in the PDE δ receptors. For the **7b**_5X74, **7b**_4jvb, and **7b**_5e80 complexes, the highest RMSF values were observed in the loop amino acid residues

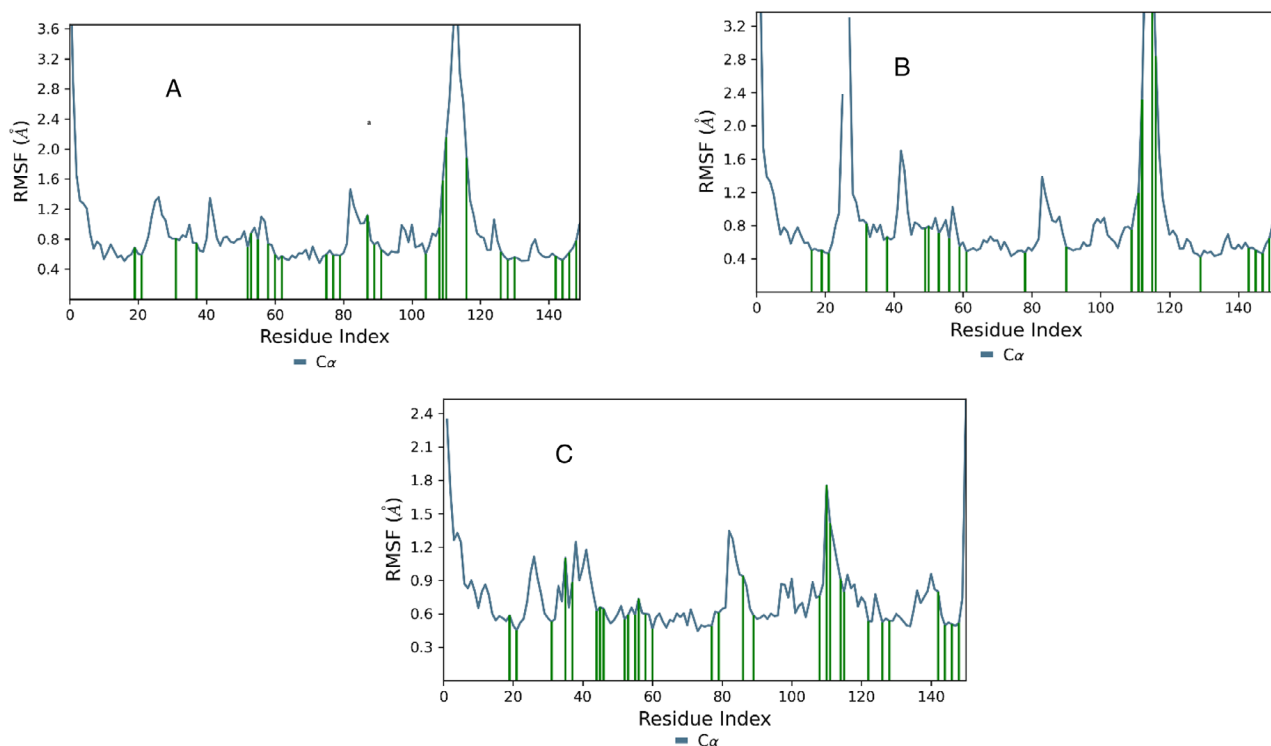


FIGURE 5 | Protein RMSF profiles of the compounds and B-factor of residues: (A) **7b**_5X74, (B) **7b**_4jvb, and (C) **7b**_5e80 in the phosphodiesterase delta PDE δ active sites during 100 nm MD simulation.

Ala111–Met118 and found to be 3.6, 3.2, and 1.8 Å, respectively, as depicted in Figure 5. Overall, the fluctuation profiles of the three complexes are predominantly observed in the loop regions of the PDE δ receptors. This observation aligns with previous MD simulations of the PDE δ receptor, which also reported significant fluctuations in these same loop regions [53].

4.3 | Protein–Ligand Interactions

Throughout the simulation period, the interactions between compound **7b** and the three PDE δ receptors were continuously monitored. These interactions are classified into four categories: hydrogen bonds, ionic interactions, hydrophobic contacts, and water bridges and are presented in Figure 6A,B.

In drug design, hydrogen bonds play a crucial role in ligand binding and significantly influence drug selectivity, metabolism, and absorption. The current in silico study demonstrated that the Hesp docking conformation is capable of forming a hydrogen bond and adopting a favorable orientation with the binding pocket residues involved in ligand interactions. In the **7b**_5X74 complex, hydrogen bonds were observed between the protein and ligand, specifically between Gln78 and the N-1 atom, and Arg61 and the N-3 atom of the triazine backbone, with occupancies of up to 88% and 63%, respectively. Notably, a persistent hydrogen bond was formed between Arg61 and the N-3 atom that maintained 100% of the time during complexation with the PDE δ receptor. In addition, compound **7b** formed a hydrogen bond with the amino acid Arg61 through the N-1 atom of the triazine moiety for up to 99% of the simulation time within the 5e80 active site (Figure 6C). This finding aligns with our docking studies, which highlighted the importance of the Arg61 residue in hydrogen

bond formation, and is also consistent with a previous simulation study involving PDE δ receptors [54]. In addition, hydrophobic contact points involving amino acid residues such as Val159, Val80, Trp90, Ile129, Ala111, and Leu147 were observed to interact with the aromatic or aliphatic groups of the ligand, as shown in Figure 6A–C. These nonpolar interactions play a critical role in maintaining the stability of the complex throughout the simulation. Overall, the consistent hydrophobic interactions observed for compound **7b** particularly in the 5e80 system suggest that hydrophobic forces are the primary contributors to the stabilization of receptor–inhibitor complexes. Moreover, water bridges represent hydrogen-bonded interactions between the protein and ligand **7b**, mediated by a water molecule.

4.4 | Ligand **7b** Torsion Profile

The ligand torsion histograms for the **7b** complex (PDB: 5e80) depict the structural evolution of each rotatable bond (RB) throughout the simulation (0.00–100.5 ns), as illustrated in Figure 7A,B. The 2D structure of ligand **7b**_5e80, with color-coded RBs, is shown alongside corresponding radial (dial) and bar plots of torsion angles in Figure 7A. The radial plots capture the distribution of torsional conformations across the simulation timeline. Ligand **7b**_5e80 displayed notable flexibility within the allosteric site, particularly in the –OH side groups, which underwent significant torsional rotations. These observations provide insights into conformational strain contributing to the stabilization of the ligand's bound state (Figure 7B). In addition, the ligand exhibits fluctuations in its properties during the initial and intermediate stages of the simulation but gradually stabilizes, returning to equilibrium over the course of 100 ns, indicating its stability within the protein's active site.

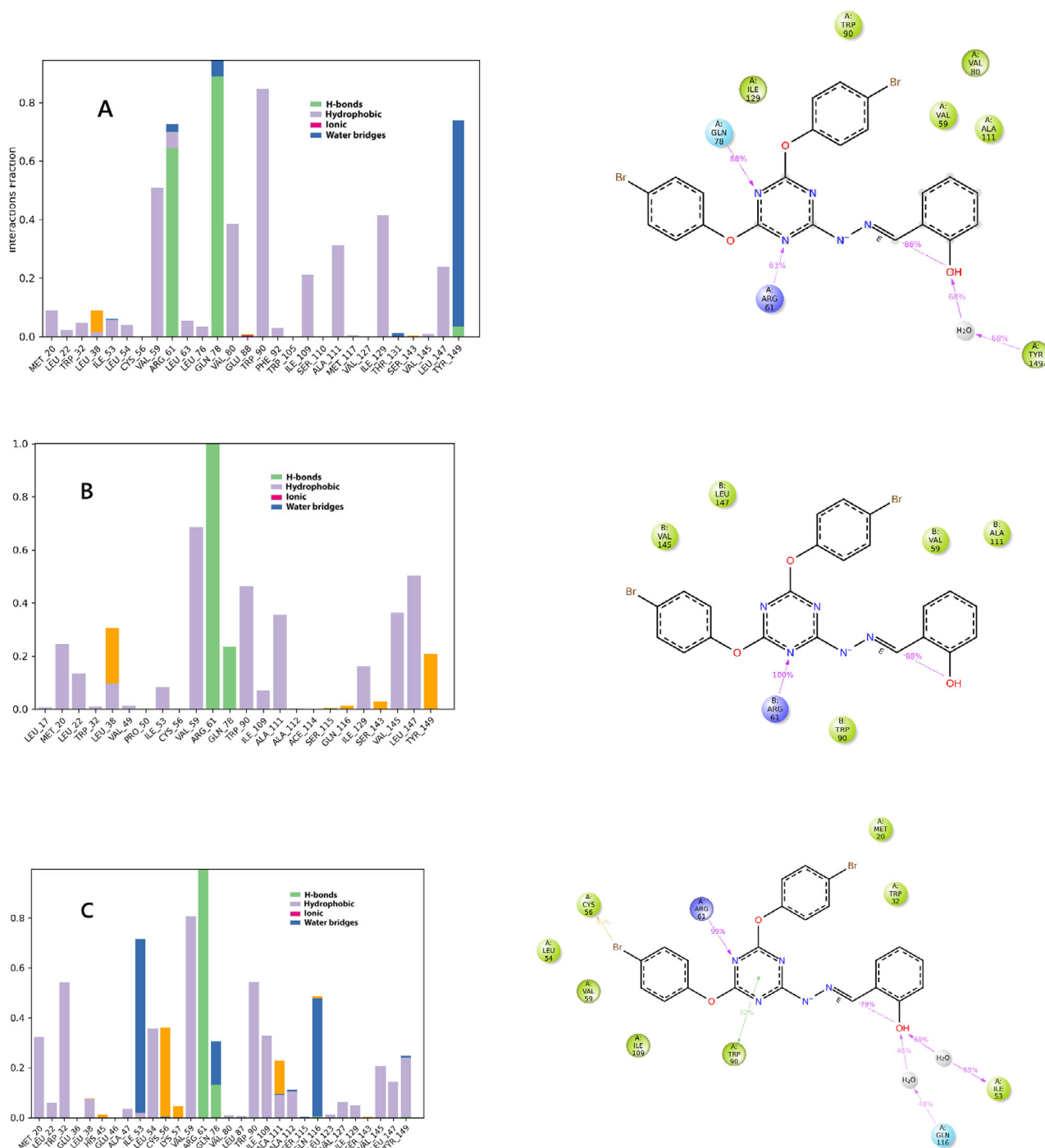


FIGURE 6 | Analysis of the molecular interactions and contact types between compound **7b** and its target receptors following MD simulations: (A) Interaction type chart and detailed 2D schematic representation with the 5X74 receptor. (B) Interaction type chart and detailed 2D schematic representation with the 4jvb receptor. (C) Interaction type chart and detailed 2D schematic representation with the 5e80 receptor.

5 | Experimental

5.1 | Materials

Cyanuric chloride was purchased from Sigma-Aldrich (Switzerland). Phenol, cinnamaldehyde, 4-chlorophenol, 4-methoxyphenol, and 4-bromophenol were procured from Merck (Darmstadt, Germany). Anhydrous potassium carbonate was the product of Unichem (Mumbai, India). Hydrazine monohydrate (98%), benzophenone, and *p*-

cresol were purchased from Fluka (Steinheim, Germany), whereas 3-nitrobenzaldehyde and 4-nitrobenzaldehyde were the products of Richest group Ltd. (Shanghai, China). Benzaldehyde, tetrahydrofuran, 2-hydroxybenzaldehyde, 3-hydroxybenzaldehyde, 4-hydroxybenzaldehyde, 4-(*N,N*-dimethylamino)benzaldehyde, pyridine-3-carboxaldehyde, and pyridine-4-carboxaldehyde were purchased from Sigma-Aldrich (St. Louis, MO, USA). Vanillin, *p*-tolualdehyde, *p*-anisaldehyde 3-chlorobenzaldehyde, and 4-chlorobenzaldehyde were supplied by Aldrich (Steinheim, Germany). Absolute ethanol, chloroform,

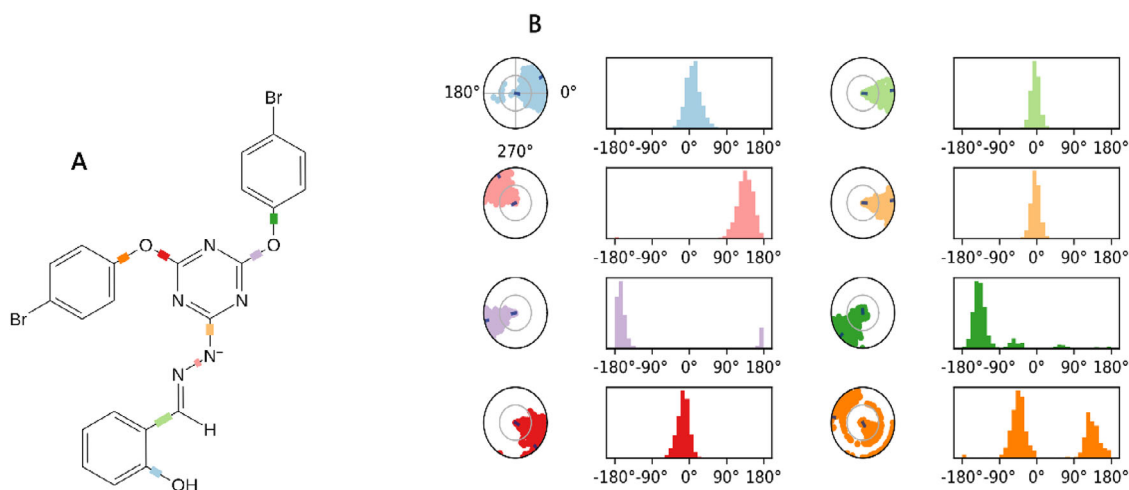


FIGURE 7 | Ligand torsion profile of the **7b** complex (PDB: 5e80): (A) torsion and flexibility and (B) ligand torsion angles.

and 1,4-dioxane were purchased from E. Merck (Darmstadt, Germany), while *n*-hexane, acetone, methanol, and ethyl acetate were obtained from commercial sources and distilled before use.

5.2 | General Experimental Methods

Melting points were determined using a Stuart SMP3 melting point apparatus and are uncorrected. NMR spectra were recorded on a Bruker Avance 300 MHz spectrometer (Bruker, Switzerland) at 300 MHz (^1H) and 75 MHz (^{13}C), are reported on the δ scale in ppm. IR spectra were obtained on a Thermo Scientific Nicolet 6700 FTIR spectrophotometer using the ATR mode. UV/Vis spectra were measured on a UV-Genesys 30 spectrophotometer (Thermo Fischer Scientific Inc.). HRMS were acquired on a quadrupole time-of-flight (QTOF) mass spectrometer (Agilent Technologies). Reactions were monitored using thin-layer chromatography (TLC) on silica gel plates 60 F_{254} coated on aluminum sheets (Merck, Germany). Chromatograms were visualized under UV light (254–366 nm) and iodine, with CHCl_3 :MeOH (9:1) as a solvent.

5.2.1 | General Procedure for the Synthesis of 1,3,5-Triazine-Hydrazone Derivatives 2a–e

2-Hydrazino-4,6-disubstituted-1,3,5-triazine derivatives **2a–e** were synthesized first following the synthetic strategy and methods reported by Barakat et al. [28].

5.2.2 | General Procedure for the Synthesis of 2-(2-(Arylbenzylidenehydrazinyl)-4,6-(Substituted-Diphenoxy)-1,3,5-Triazines 3a–o to 7a–o

The respective **2a–e** (0.01 mol) was added to dry EtOH (20 mL) and the mixture stirred for 15 min at room temperature, followed by the addition of substituted benzaldehyde (0.012 mol) and catalytic amounts of NaHSO_3 . The reaction mixture was heated under reflux for 6–12 h, a solid product separated in the reaction

mixture. On the completion of reaction as indicated by TLC, the reaction mixture was filtered, washed with cold EtOH, and recrystallized from MeCN–EtOH to afford the pure product.

5.2.2.1 | 2-(2-(Benzylidenehydrazinyl)-4,6-Diphenoxy-1,3,5-Triazine (3a). Yield: 87%; mp: 230°C–232°C [Lit. 230°C–231°C] [36]; R_f : 0.71. IR (ATR, $\bar{\nu}$): 3234 (NH), 3055 ($\text{C}_{\text{sp}2}\text{—H}_{\text{stretch.}}$), 1612 ($\text{C}=\text{N}$), 1568, 1491 ($2 \times \text{C}=\text{C}$), 1368, 1201 ($2 \times \text{C—O}_{\text{stretch.}}$) cm^{-1} . ^1H NMR (300 MHz, $\text{DMSO-}d_6$): δ 11.83 (1H, s, NH), 8.17 (1H, s, $\text{H—C}=\text{N}$), 7.64–7.62 (2H, m, ArH), 7.48–7.41 (7H, m, ArH), 7.29–7.23 (6H, m, ArH). ^{13}C NMR (75 MHz, $\text{DMSO-}d_6$): δ 172.8, 172.0, 166.9 ($3 \times \text{C-triazine}$), 146.3 ($\text{H—C}=\text{N}$), 152.2, 134.7, 130.3, 130.0, 129.8, 129.2, 127.3, 126.1, 126.0, 122.2, 122.1 (11 \times ArC). HRMS (ESI): m/z calcd for $\text{C}_{22}\text{H}_{17}\text{N}_5\text{O}_2 + \text{H}^+$: 384.1460 [$\text{M} + \text{H}$] $^+$; found: 384.1451.

5.2.2.2 | 2-(2-(2-Hydroxybenzylidene)Hydrazinyl)-4,6-Diphenoxy-1,3,5-Triazine (3b). Yield: 90%; mp: 224°C–226°C; R_f : 0.55. IR (ATR, $\bar{\nu}$): 3350–2900 (br., OH), 3223 (NH), 3008 ($\text{C}_{\text{sp}2}\text{—H}_{\text{stretch.}}$), 1619 ($\text{C}=\text{N}$), 1565, 1488 ($2 \times \text{C}=\text{C}$), 1368, 1194 ($2 \times \text{C—O}_{\text{stretch.}}$) cm^{-1} . ^1H NMR (300 MHz, $\text{DMSO-}d_6$): δ 12.10 (1H, s, NH), 10.93 (1H, s, OH), 8.33 (1H, s, $\text{H—C}=\text{N}$), 7.48–7.40 (5H, m, ArH), 7.29–7.24 (7H, m, ArH), 6.90–6.58 (2H, m, ArH). ^{13}C NMR (75 MHz, $\text{DMSO-}d_6$): δ 172.7, 172.1, 166.5 ($3 \times \text{C-triazine}$), 147.1 ($\text{H—C}=\text{N}$), 157.7, 152.2, 152.1, 131.6, 130.1, 129.9, 126.1, 122.1, 119.7, 118.9, 116.9 (11 \times ArC). HRMS (ESI): m/z calcd for $\text{C}_{22}\text{H}_{17}\text{N}_5\text{O}_3 + \text{H}^+$: 400.1410 [$\text{M} + \text{H}$] $^+$; found: 400.1402.

5.2.2.3 | 2-(2-(3-Hydroxybenzylidene)Hydrazinyl)-4,6-Diphenoxy-1,3,5-Triazine (3c). Yield: 89%; mp: 258°C–260°C; R_f : 0.50. IR (ATR, $\bar{\nu}$): 3400–3000 (br., OH), 3232 (NH), 3062 ($\text{C}_{\text{sp}2}\text{—H}_{\text{stretch.}}$), 1612 ($\text{C}=\text{N}$), 1571, 1544 ($2 \times \text{C}=\text{C}$), 1368, 1191 ($2 \times \text{C—O}_{\text{stretch.}}$) cm^{-1} . ^1H NMR (300 MHz, $\text{DMSO-}d_6$): δ 11.79 (1H, s, NH), 9.63 (1H, s, OH), 7.44 (1H, s, $\text{H—C}=\text{N}$), 7.44–7.42 (4H, m, ArH), 7.27–7.14 (8H, m, ArH), 7.00 (1H, d, $J = 6.6$ Hz, ArH), 6.80 (1H, d, $J = 6.6$ Hz, ArH). ^{13}C NMR (75 MHz, $\text{DMSO-}d_6$): δ 172.8, 171.9, 166.9 ($3 \times \text{C-triazine}$), 146.5 ($\text{H—C}=\text{N}$), 158.1, 152.2, 135.9, 130.3, 130.0, 129.8, 126.1, 122.2, 119.0, 117.7, 112.9 (11 \times ArC). HRMS (ESI): m/z calcd for $\text{C}_{22}\text{H}_{17}\text{N}_5\text{O}_3 + \text{H}^+$: 400.1410 [$\text{M} + \text{H}$] $^+$; found: 400.1495.

5.2.2.4 | 2-(2-(4-Hydroxybenzylidene)hydrazinyl)-4,6-diphenoxy-1,3,5-triazine (3d). Yield: 80%; mp: 160°C–162°C; R_f : 0.49. IR (ATR, $\bar{\nu}$): 3500–3000 (br., OH), 3235 (NH), 3060 ($C_{sp2}-H_{stretch.}$), 1598 (C=N), 1571, 1491 ($2 \times C=C$), 1369, 1212 ($2 \times C-O_{stretch.}$) cm^{-1} . 1H NMR (300 MHz, DMSO- d_6): δ 11.64 (1H, s, NH), 9.92 (1H, s, OH), 8.07 (1H, s, H-C=N), 7.47–7.39 (6H, m, ArH), 7.30–7.21 (6H, m, ArH), 6.79 (2H, d, $J = 8.7$ Hz, ArH); ^{13}C NMR (75 MHz, DMSO- d_6): δ 172.7, 171.9, 166.6 ($3 \times C$ -triazine), 146.7 (H-C=N), 159.7, 152.2, 130.0, 129.8, 129.1, 126.1, 126.0, 125.7, 122.3, 122.2, 116.1 ($11 \times ArC$). HRMS (ESI): m/z calcd for $C_{22}H_{17}N_5O_3 + H^+$: 400.1410 [M + H] $^+$; found: 400.1401.

5.2.2.5 | 2-(2-(4-Methoxybenzylidene)hydrazinyl)-4,6-Diphenoxy-1,3,5-Triazine (3e). Yield: 91%; mp: 209°C–212°C; R_f : 0.76. IR (ATR, $\bar{\nu}$): 3241 (NH), 3055 ($C_{sp2}-H_{stretch.}$), 2842 ($C_{sp3}-H_{stretch.}$), 1610 (C=N), 1572, 1492 ($2 \times C=C$), 1374, 1211 ($2 \times C-O_{stretch.}$) cm^{-1} . 1H NMR (300 MHz, DMSO- d_6): δ 11.70 (1H, s, NH), 8.11 (1H, s, H-C=N), 7.56 (2H, d, $J = 8.7$ Hz, ArH), 7.44–7.39 (4H, m, ArH), 7.29–7.22 (6H, m, ArH), 6.97 (2H, d, $J = 8.7$ Hz, ArH), 3.79 (3H, s, OCH $_3$). ^{13}C NMR (75 MHz, DMSO- d_6): δ 172.7, 171.9, 166.7, 161.1 ($3 \times C$ -triazine), 146.3 (H-C=N), 152.2, 130.0, 129.8, 128.9, 127.2, 126.1, 126.0, 122.2, 122.1, 114.7 ($10 \times ArC$). HRMS (ESI): m/z calcd for $C_{23}H_{19}N_5O_3 + Na^+$: 436.1386 [M + Na] $^+$; found: 436.1373.

5.2.2.6 | 2-(2-(4-Methylbenzylidene)Hydrazinyl)-4,6-Diphenoxy-1,3,5-Triazine (3f). Yield: 85%; mp: 208°C–211°C; R_f : 0.77. IR (ATR, $\bar{\nu}$): 3239 (NH), 3057 ($C_{sp2}-H_{stretch.}$), 2910 ($C_{sp3}-H_{stretch.}$), 1614 (C=N), 1573, 1492 ($2 \times C=C$), 1372, 1215 ($2 \times C-O_{stretch.}$) cm^{-1} . 1H NMR (300 MHz, CDCl $_3$): δ 8.92 (1H, s, NH), 7.88 (1H, s, H-C=N), 7.58 (2H, d, $J = 8.1$ Hz, ArH), 7.41–7.36 (4H, m, ArH), 7.28–7.13 (9H, m, ArH), 2.38 (3H, s, CH $_3$). ^{13}C NMR (75 MHz, CDCl $_3$): δ 173.0, 171.9, 166.5 ($3 \times C$ -triazine), 146.5 (H-C=N), 151.8, 140.8, 130.6, 130.1, 129.8, 129.3, 127.6, 125.7, 121.6 ($9 \times ArC$), 21.5 (CH $_3$). HRMS (ESI): m/z calcd for $C_{23}H_{19}N_5O_2 + Na^+$: 420.1436 [M + Na] $^+$; found: 420.1411.

5.2.2.7 | 2-(2-(4-*N,N*-Dimethylaminobenzylidene)Hydrazinyl)-4,6-Diphenoxy-1,3,5-Triazin (3g). Yield: 95%; mp: 233°C–234°C; R_f : 0.77. IR (ATR, $\bar{\nu}$): 3240 (NH), 3137 ($C_{sp2}-H_{stretch.}$), 1600 (C=N), 1570, 1487 ($2 \times C=C$), 1367, 1178 ($2 \times C-O_{stretch.}$) cm^{-1} . 1H NMR (300 MHz, DMSO- d_6): δ 11.55 (1H, s, NH), 8.04 (1H, s, H-C=N), 7.47–7.39 (6H, m, ArH), 7.30–7.21 (6H, m, ArH), 6.71 (2H, d, $J = 8.7$ Hz, ArH), 2.96 (6H, s, $2 \times CH_3$). ^{13}C NMR (75 MHz, DMSO- d_6): δ 172.7, 171.8, 166.4 ($3 \times C$ -triazine), 147.3 (H-C=N), 152.2, 151.8, 130.0, 129.8, 128.7, 126.0, 125.9, 122.3, 122.2, 121.9, 112.2 ($11 \times ArC$). HRMS (ESI): m/z calcd for $C_{24}H_{22}N_6O_2 + H^+$: 427.1882 [M + H] $^+$; found: 427.1863.

5.2.2.8 | 4,6-Diphenoxy-2-(2-((*E*)-3-Phenylallylidene)-1,3,5-Triazine (3h). Yield: 95%; mp: 226°C–228°C; R_f : 0.65. IR (ATR, $\bar{\nu}$): 3222 (NH), 3099 ($C_{sp2}-H_{stretch.}$), 1625 (C=N), 1587, 1488 ($2 \times C=C$), 1365, 1196 ($2 \times C-O_{stretch.}$) cm^{-1} . 1H NMR (300 MHz, CDCl $_3$): δ 9.21 (1H, s, NH), 7.80–7.77 (1H, d, $J = 9.3$ Hz, H-C=N), 7.41–7.28 (7H, m, ArH), 7.23–7.04 (9H, m, ArH, CH=CHAr), 6.71 (1H, d, $J = 16.2$ Hz, CH=CHAr). ^{13}C NMR (75 MHz, CDCl $_3$): δ 172.8, 171.9, 166.7 ($3 \times C$ -triazine), 148.9 (H-C=N), 136.3 (CH=CHAr), 152.2, 139.3, 130.0, 129.9, 129.4, 129.2, 127.5, 126.1, 126.0, 122.1 ($10 \times ArC$), 125.7 (CH=CHAr). HRMS (ESI): m/z calcd for $C_{24}H_{19}N_5O_2 + Na^+$: 432.1436 [M + Na] $^+$; found: 432.1420.

5.2.2.9 | 2-(2-(4-Hydroxy-3-Methoxybenzylidene)Hydrazinyl)-4,6-Diphenoxy-1,3,5-Triazine (3i). Yield: 80%; mp: 228°C–229°C; R_f : 0.63. IR (ATR, $\bar{\nu}$): 3414 (br., OH), 3232 (NH), 3054 ($C_{sp2}-H_{stretch.}$), 2945 ($C_{sp3}-H_{stretch.}$), 1609 (C=N), 1571, 1516 ($2 \times C=C$), 1367, 1193 ($2 \times C-O_{stretch.}$) cm^{-1} . 1H NMR (300 MHz, DMSO- d_6): δ 11.67 (1H, s, NH), 9.54 (1H, s, OH), 8.02 (1H, s, H-C=N), 7.44–7.41 (4H, m, ArH), 7.29–7.23 (6H, m, ArH), 7.15 (1H, s, ArH), 6.95 (1H, d, $J = 7.8$ Hz, ArH), 6.78 (1H, d, $J = 8.1$ Hz, ArH), 3.75 (3H, s, OCH $_3$). ^{13}C NMR (75 MHz, DMSO- d_6): δ 172.7, 172.0, 166.5 ($3 \times C$ -triazine), 146.6 (H-C=N), 152.2, 149.2, 148.4, 130.0, 129.7, 126.1, 125.9, 122.4, 122.3, 122.2, 115.7, 108.7 ($12 \times ArC$), 55.8 (OCH $_3$). HRMS (ESI): m/z calcd for $C_{23}H_{19}N_5O_4 + H^+$: 430.1515 [M + H] $^+$; found: 430.1504.

5.2.2.10 | 2-(2-(3-Chlorobenzylidene)Hydrazinyl)-4,6-Diphenoxy-1,3,5-Triazine (3j). Yield: 83%; mp: 230°C–231°C; R_f : 0.87. IR (ATR, $\bar{\nu}$): 3235 (NH), 3055 ($C_{sp2}-H_{stretch.}$), 1613 (C=N), 1570, 1492 ($2 \times C=C$), 1372, 1208 ($2 \times C-O_{stretch.}$) cm^{-1} . 1H NMR (300 MHz, DMSO- d_6): δ 11.98 (1H, s, NH), 8.13 (1H, s, H-C=N), 7.67 (1H, s, ArH), 7.57–7.54 (1H, m, ArH), 7.45–7.41 (6H, m, ArH), 7.30–7.23 (6H, m, ArH). ^{13}C NMR (75 MHz, DMSO- d_6): δ 172.8, 172.1, 167.0 ($3 \times C$ -triazine), 144.3 (H-C=N), 152.2, 136.9, 134.1, 131.1, 130.0, 129.9, 129.8, 126.3, 126.2, 122.3, 122.2 ($11 \times ArC$). HRMS (ESI): m/z calcd for $C_{22}H_{16}ClN_5O_2 + Na^+$: 440.0890 [M + Na] $^+$; found: 440.0879.

5.2.2.11 | 2-(2-(4-Chlorobenzylidene)Hydrazinyl)-4,6-Diphenoxy-1,3,5-Triazine (3k). Yield: 68%; mp: 250°C–252°C; R_f : 0.79. IR (ATR, $\bar{\nu}$): 3236 (NH), 3054 ($C_{sp2}-H_{stretch.}$), 1597 (C=N), 1569, 1490 ($2 \times C=C$), 1368, 1203 ($2 \times C-O_{stretch.}$) cm^{-1} . 1H NMR (300 MHz, DMSO- d_6): δ 11.90 (1H, s, NH), 8.15 (1H, s, H-C=N), 7.64 (2H, d, $J = 9.0$ Hz, ArH), 7.50–7.40 (6H, m, ArH), 7.29–7.22 (6H, m, ArH). ^{13}C NMR (75 MHz, DMSO- d_6): δ 172.8, 172.0, 167.0 ($3 \times C$ -triazine), 144.9 (H-C=N), 152.2, 134.7, 133.6, 130.0, 129.8, 129.3, 128.9, 126.1, 122.2, 122.1 ($10 \times ArC$). HRMS (ESI): m/z calcd for $C_{22}H_{16}ClN_5O_2 + Na^+$: 440.0890 [M + Na] $^+$; found: 440.0884.

5.2.2.12 | 2-(2-(3-Nitrobenzylidene)Hydrazinyl)-4,6-Diphenoxy-1,3,5-Triazine (3l). Yield: 70%; mp: 210°C–212°C; R_f : 0.58. IR (ATR, $\bar{\nu}$): 3216 (NH), 3109 ($C_{sp2}-H_{stretch.}$), 1611 (C=N), 1566, 1523 ($2 \times C=C$), 1366, 1189 ($2 \times C-O_{stretch.}$) cm^{-1} . 1H NMR (300 MHz, DMSO- d_6): δ 12.10 (1H, s, NH), 8.44 (1H, s, H-C=N), 8.26–8.21 (2H, m, ArH), 8.02 (1H, d, $J = 7.2$ Hz, ArH), 7.70 (1H, t, $J = 7.8$ Hz, ArH), 7.46–7.42 (4H, m, ArH), 7.31–7.24 (6H, m, ArH). ^{13}C NMR (75 MHz, DMSO- d_6): δ 172.8, 172.1, 167.1 ($3 \times C$ -triazine), 143.7 (H-C=N), 152.1, 148.6, 136.5, 133.7, 130.9, 130.1, 129.8, 126.2, 124.4, 122.2, 120.9 ($11 \times ArC$). HRMS (ESI): m/z calcd for $C_{22}H_{16}N_6O_4 + Na^+$: 451.1131 [M + Na] $^+$; found: 451.1120.

5.2.2.13 | 2-(2-(4-Nitrobenzylidene)Hydrazinyl)-4,6-Diphenoxy-1,3,5-Triazine (3m). Yield: 73%; mp: 256°C–258°C; R_f : 0.58. IR (ATR, $\bar{\nu}$): 3236 (NH), 3057 ($C_{sp2}-H_{stretch.}$), 1613 (C=N), 1564, 1521 ($2 \times C=C$), 1345, 1204 ($2 \times C-O_{stretch.}$) cm^{-1} . 1H NMR (300 MHz, DMSO- d_6): δ 12.14 (1H, s, NH), 8.25 (3H, m, ArH), 7.87 (2H, d, $J = 9.0$ Hz, ArH), 7.49–7.41 (4H, m, ArH), 7.31–7.24 (6H, m, ArH). ^{13}C NMR (75 MHz, DMSO- d_6): δ 172.8, 172.1, 167.2 ($3 \times C$ -triazine), 141.0 (H-C=N), 152.1, 148.0, 143.6, 130.1, 129.8, 128.1, 126.1, 124.5, 122.2, 122.1 ($10 \times ArC$). HRMS (ESI): m/z calcd for $C_{22}H_{16}N_6O_4 + Na^+$: 451.1131 [M + Na] $^+$; found: 451.1118.

5.2.2.14 | 4,6-Diphenoxy-2-(2-(Pyridin-3-

Ylmethylene)Hydrazinyl)-1,3,5-Triazine (3n). Yield: 90%; mp: 234°C–236°C; R_f : 0.63. IR (ATR, $\bar{\nu}$): 3231 (NH), 3054 (C_{sp2} –H_{stretch.}), 1621 (C=N), 1562, 1491 ($2 \times C=C$), 1361, 1211 ($2 \times C$ –O_{stretch.}) cm^{-1} . 1H NMR (300 MHz, DMSO- d_6): δ 12.00 (1H, s, NH), 8.75 (1H, d, $J = 1.5$ Hz, ArH), 8.57 (1H, dd, $J = 4.8$, 1.5 Hz, ArH), 8.20 (1H, s, H–C=N), 8.01 (1H, dt, $J = 8.1$, 1.8 Hz, ArH), 7.47–7.43 (5H, m, ArH), 7.29–7.23 (6H, m, ArH). ^{13}C NMR (75 MHz, DMSO- d_6): δ 172.8, 172.1, 167.0 ($3 \times C$ -triazine), 143.4 (H–C=N), 152.2, 150.9, 148.8, 133.7, 130.6, 130.0, 129.8, 126.1, 124.4, 122.1 ($10 \times ArC$). HRMS (ESI): m/z calcd for $C_{21}H_{16}N_6O_2 + H^+$: 385.1413 [M + H] $^+$; found: 385.1405.

5.2.2.15 | 4,6-Diphenoxy-2-(2-(Pyridin-4-

Ylmethylene)Hydrazinyl)-1,3,5-Triazine (3o). Yield: 92%; mp: 274°C–276°C; R_f : 0.53. IR (ATR, $\bar{\nu}$): 3232 (NH), 3049 (C_{sp2} –H_{stretch.}), 1616 (C=N), 1574, 1490 ($2 \times C=C$), 1362, 1213 ($2 \times C$ –O_{stretch.}) cm^{-1} . 1H NMR (300 MHz, DMSO- d_6): δ 12.13 (1H, s, NH), 8.14 (1H, s, H–C=N), 8.61 (2H, d, $J = 5.4$ Hz, ArH), 7.55 (2H, d, $J = 5.7$ Hz, ArH), 7.46–7.41 (4H, m, ArH), 7.30–7.24 (6H, m, ArH). ^{13}C NMR (75 MHz, DMSO- d_6): δ 172.8, 172.1, 167.1 ($3 \times C$ -triazine), 143.6 (H–C=N), 152.1, 150.6, 141.8, 130.1, 129.8, 126.2, 122.2, 121.2 ($8 \times ArC$). HRMS (ESI): m/z calcd for $C_{21}H_{16}N_6O_2 + H^+$: 385.1413 [M + H] $^+$; found: 385.1401.

5.2.2.16 | 2-(2-(Benzylidenehydrazinyl)-4,6-Bis(4-

Methoxyphenoxy)-1,3,5-Triazine (4a). Yield: 72%; mp: 188°C–190°C; R_f : 0.68. IR (ATR, $\bar{\nu}$): 3236 (NH), 3118 (C_{sp2} –H_{stretch.}), 2833 (C_{sp3} –H_{stretch.}), 1608 (C=N), 1577, 1503 ($2 \times C=C$), 1373, 1203 ($2 \times C$ –O_{stretch.}) cm^{-1} . 1H NMR (300 MHz, $CDCl_3$): δ 9.20 (1H, s, NH), 7.91 (1H, s, H–C=N), 7.70–7.64 (2H, m, ArH), 7.38–7.34 (3H, m, ArH), 7.12–7.05 (4H, m, ArH), 6.88 (4H, d, $J = 7.8$ Hz, ArH), 3.80 (6H, s, $2 \times OCH_3$). ^{13}C NMR (75 MHz, $CDCl_3$): δ 173.1, 172.3, 166.9 ($3 \times C$ -triazine), 145.7 (H–C=N), 157.2, 146.1, 134.7, 130.3, 129.2, 127.3, 123.1, 123.0, 114.9, 114.7 ($10 \times ArC$), 55.9 (OCH_3). HRMS (ESI): m/z calcd for $C_{24}H_{21}N_5O_4 + H^+$: 444.1672 [M + H] $^+$; found: 444.1661.

5.2.2.17 | 2-(2-(2-Hydroxybenzylidene)Hydrazinyl)-4,6-

Bis(4-Methoxyphenoxy)-1,3,5-Triazine (4b). Yield: 70%; mp: 219°C–221°C; R_f : 0.76. IR (ATR, $\bar{\nu}$): 3300–2750 (br., OH), 3218 (NH), 3095 (C_{sp2} –H_{stretch.}), 2838 (C_{sp3} –H_{stretch.}), 1598 (C=N), 1572, 1499 ($2 \times C=C$), 1366, 1195 ($2 \times C$ –O_{stretch.}) cm^{-1} . 1H NMR (300 MHz, DMSO- d_6): δ 12.05 (1H, s, NH), 10.94 (1H, s, OH), 8.32 (1H, s, H–C=N), 7.39 (1H, dd, $J = 8.1$, 1.5 Hz, ArH), 7.29–7.24 (1H, m, ArH), 7.19–7.14 (4H, m, ArH), 6.99–6.95 (4H, m, ArH), 6.90–6.85 (2H, m, ArH), 3.76 (3H, s, OCH_3), 3.74 (3H, s, OCH_3). ^{13}C NMR (75 MHz, DMSO- d_6): δ 173.1, 172.5, 166.4 ($3 \times C$ -triazine), 145.6 (H–C=N), 157.7, 157.3, 157.2, 147.1, 131.6, 130.1, 123.0, 122.9, 119.7, 118.9, 116.9, 115.0, 114.9 ($13 \times ArC$), 55.9 ($2 \times OCH_3$). HRMS (ESI): m/z calcd for $C_{25}H_{21}N_5O_5 + H^+$: 460.1621 [M + H] $^+$; found: 460.1611.

5.2.2.18 | 2-(2-(3-Hydroxybenzylidene)Hydrazinyl)-4,6-

Bis(4-Methoxyphenoxy)-1,3,5-Triazine (4c). Yield: 73%; mp: 245°C–247°C; R_f : 0.76. IR (ATR, $\bar{\nu}$): 3400–2900 (br., OH), 3221 (NH), 3061 (C_{sp2} –H_{stretch.}), 2829 (C_{sp3} –H_{stretch.}), 1606 (C=N), 1570, 1500 ($2 \times C=C$), 1372, 1188 ($2 \times C$ –O_{stretch.}) cm^{-1} . 1H NMR (300 MHz, DMSO- d_6): δ 11.72 (1H, s, NH), 9.63 (1H, s, OH), 8.06 (1H, s, H–C=N), 7.24–7.13 (6H, m, ArH), 7.01–6.93 (5H, m, ArH), 6.80 (1H, dd, $J = 8.1$, 1.8 Hz, ArH), 3.78 (3H, s, OCH_3), 3.75 (3H,

s, OCH_3). ^{13}C NMR (75 MHz, DMSO- d_6): δ 173.1, 172.3, 166.9 ($3 \times C$ -triazine), 145.6 (H–C=N), 158.1, 157.2, 146.3, 136.0, 130.2, 123.0, 119.0, 117.7, 114.9, 114.7, 112.9 ($11 \times ArC$), 55.9 ($2 \times OCH_3$). HRMS (ESI): m/z calcd for $C_{25}H_{21}N_5O_5 + H^+$: 460.1621 [M + H] $^+$; found: 460.1609.

5.2.2.19 | 2-(2-(4-Hydroxybenzylidene)Hydrazinyl)-4,6-

Bis(4-Methoxyphenoxy)-1,3,5-Triazine (4d). Yield: 70%; mp: 206°C–208°C; R_f : 0.76. IR (ATR, $\bar{\nu}$): 3400–2800 (br., OH), 3232 (NH), 3005 (C_{sp2} –H_{stretch.}), 2833 (C_{sp3} –H_{stretch.}), 1602 (C=N), 1573, 1504 ($2 \times C=C$), 1370, 1196 ($2 \times C$ –O_{stretch.}) cm^{-1} . 1H NMR (300 MHz, DMSO- d_6): δ 11.58 (1H, s, NH), 9.94 (1H, s, OH), 8.06 (1H, s, H–C=N), 7.45 (2H, d, $J = 8.7$ Hz, ArH), 7.19–7.12 (4H, m, ArH), 6.99–6.93 (4H, m, ArH), 6.79 (2H, d, $J = 8.7$ Hz, ArH), 3.78 (3H, s, OCH_3), 3.75 (3H, s, OCH_3). ^{13}C NMR (75 MHz, DMSO- d_6): δ 173.1, 172.2, 166.6 ($3 \times C$ -triazine), 146.5 (H–C=N), 159.7, 157.2, 157.1, 145.7, 145.6, 129.1, 125.7, 123.1, 123.0, 116.1, 114.9, 114.7 ($12 \times ArC$), 55.9 ($2 \times OCH_3$). HRMS (ESI): m/z calcd for $C_{25}H_{21}N_5O_5 + H^+$: 460.1621 [M + H] $^+$; found: 460.1617.

5.2.2.20 | 2-(2-(4-Methoxybenzylidene)Hydrazinyl)-

4,6-Bis(4-Methoxyphenoxy)-1,3,5-Triazine (4e). Yield: 70%; mp: 291°C–293°C; R_f : 0.65. IR (ATR, $\bar{\nu}$): 3232 (NH), 3008 (C_{sp2} –H_{stretch.}), 2837 (C_{sp3} –H_{stretch.}), 1604 (C=N), 1569, 1503 ($2 \times C=C$), 1366, 1192 ($2 \times C$ –O_{stretch.}) cm^{-1} . 1H NMR (300 MHz, DMSO- d_6): δ 11.65 (1H, s, NH), 8.11 (1H, s, H–C=N), 7.56 (2H, d, $J = 8.7$ Hz, ArH), 7.20–7.12 (4H, m, ArH), 6.99–6.93 (6H, m, ArH), 3.79 (3H, s, OCH_3), 3.77 (3H, s, OCH_3), 3.76 (3H, s, OCH_3); ^{13}C NMR (75 MHz, DMSO- d_6): δ 173.1, 172.2, 166.6 ($3 \times C$ -triazine), 146.5 (H–C=N), 159.7, 157.1, 145.7, 129.1, 125.7, 123.1, 123.0, 116.1, 114.9, 114.7 ($10 \times ArC$), 55.9 ($3 \times OCH_3$). HRMS (ESI): m/z calcd for $C_{25}H_{23}N_5O_5 + Na^+$: 496.1597 [M + Na] $^+$; found: 496.1584.

5.2.2.21 | 4,6-Bis(4-Methoxyphenoxy)-2-(2-(4-

Methylbenzylidene)Hydrazinyl)-1,3,5-Triazine (4f). Yield: 64%; mp: 176°C–178°C; R_f : 0.65. IR (ATR, $\bar{\nu}$): 3239 (NH), 3133 (C_{sp2} –H_{stretch.}), 2835 (C_{sp3} –H_{stretch.}), 1611 (C=N), 1575, 1504 ($2 \times C=C$), 1369, 1192 ($2 \times C$ –O_{stretch.}) cm^{-1} . 1H NMR (300 MHz, DMSO- d_6): δ 11.71 (1H, s, NH), 8.13 (1H, s, H–C=N), 7.51 (2H, d, $J = 9.0$ Hz, ArH), 7.24–7.50 (6H, m, ArH), 6.99–6.90 (4H, m, ArH), 3.78 (3H, s, OCH_3), 3.76 (3H, s, OCH_3), 2.33 (3H, s, CH_3). ^{13}C NMR (75 MHz, DMSO- d_6): δ 173.1, 172.3, 166.8 ($3 \times C$ -triazine), 146.2 (H–C=N), 157.2, 145.7, 140.1, 132.0, 129.8, 127.3, 123.1, 123.0, 114.9, 114.7 ($12 \times ArC$), 55.9 ($2 \times OCH_3$), 21.4 (CH_3). HRMS (ESI): m/z calcd for $C_{25}H_{23}N_5O_4 + H^+$: 458.1828 [M + H] $^+$; found: 458.1821.

5.2.2.22 | 2-(2-(4,N,N-Dimethylaminobenzylidene)

Hydrazinyl)-4,6-Bis(4-Methoxy-Phenoxy)-1,3,5-Triazine (4g). Yield: 70%; mp: 206°C–208°C; R_f : 0.61. IR (ATR, $\bar{\nu}$): 3234 (NH), 3133 (C_{sp2} –H_{stretch.}), 2835 (C_{sp3} –H_{stretch.}), 1595 (C=N), 1550, 1504 ($2 \times C=C$), 1365, 1178 ($2 \times C$ –O_{stretch.}) cm^{-1} . 1H NMR (300 MHz, DMSO- d_6): δ 11.49 (1H, s, NH), 8.04 (1H, s, H–C=N), 7.43 (2H, d, $J = 8.7$ Hz, ArH), 7.19–7.12 (4H, m, ArH), 6.99–6.93 (4H, m, ArH), 6.71 (2H, d, $J = 8.7$ Hz, ArH), 3.78 (3H, s, OCH_3), 3.75 (3H, s, OCH_3), 2.96 (6H, s, $N(CH_3)_2$); ^{13}C NMR (75 MHz, DMSO- d_6): δ 173.0, 172.1, 166.4 ($3 \times C$ -triazine), 147.2 (H–C=N), 157.2, 157.1, 151.8, 145.7, 128.7, 123.1, 123.0, 122.0, 114.9, 114.7, 112.1 ($11 \times ArC$), 55.9 ($2 \times OCH_3$). HRMS (ESI): m/z calcd for $C_{26}H_{26}N_6O_4 + H^+$: 487.2094 [M + H] $^+$; found: 487.2082.

5.2.2.23 | 4,6-Bis(4-Methoxyphenoxy)-2-(2-((E)-3-Phenylallylidene)Hydrazinyl)-1,3,5-Triazine (4h). Yield: 70%; mp: 219°C–221°C; R_f : 0.70. IR (ATR, $\bar{\nu}$): 3235 (NH), 3055 ($C_{sp2}-H_{stretch.}$), 2836 ($C_{sp3}-H_{stretch.}$), 1627 (C=N), 1571, 1501 ($2 \times C=C$), 1368, 1176 ($2 \times C-O_{stretch.}$) cm^{-1} . 1H NMR (300 MHz, DMSO- d_6): δ 11.65 (1H, s, NH), 7.99 (1H, dd, $J = 6.6, 1.5$ Hz, H—C=N), 7.59 (2H, d, $J = 7.2$ Hz, ArH), 7.40–7.29 (3H, m, ArH), 7.17–7.13 (4H, m, ArH), 6.98–6.96 (6H, m, ArH, (CH=CHAr)), 3.77 (3H, s, OCH₃), 3.76 (3H, s, OCH₃). ^{13}C NMR (75 MHz, DMSO- d_6): δ 173.1, 172.2, 166.7 ($3 \times C$ -triazine), 145.6 (H—C=N), 157.2, 157.1, 148.8, 139.2, 129.2, 127.5, 123.0, 114.9, 114.8 ($9 \times ArC$), 136.3 (CH=CHAr), 125.8 (CH=CHAr), 55.9 ($2 \times OCH_3$). HRMS (ESI): m/z calcd for $C_{26}H_{23}N_5O_4 + H^+$: 470.1828 [M + H] $^+$; found: 470.1817.

5.2.2.24 | 2-(2-(4-Hydroxy-3-Methoxybenzylidene)Hydrazinyl)-4,6-(Bis(4-Methoxyphenoxy))-1,3,5-Triazine (4i). Yield: 68%; mp: 241°C–243°C; R_f : 0.69. IR (ATR, $\bar{\nu}$): 3412 (br., OH), 3234 (NH), 3103 ($C_{sp2}-H_{stretch.}$), 2838 ($C_{sp3}-H_{stretch.}$), 1600 (C=N), 1577, 1504 ($2 \times C=C$), 1372, 1177 ($2 \times C-O_{stretch.}$) cm^{-1} . 1H NMR (300 MHz, DMSO- d_6): δ 11.61 (1H, s, NH), 9.53 (1H, s, OH), 8.02 (1H, s, H—C=N), 7.19–7.13 (5H, m, ArH), 6.98–6.93 (5H, m, ArH), 6.78 (1H, d, $J = 8.1$ Hz, ArH), 3.77 (3H, s, OCH₃), 3.76 (3H, s, OCH₃), 3.75 (3H, s, OCH₃). ^{13}C NMR (75 MHz, DMSO- d_6): δ 173.1, 172.3, 166.5 ($3 \times C$ -triazine), 146.4 (H—C=N), 157.2, 157.1, 149.2, 148.4, 145.7, 126.1, 123.2, 123.1, 122.5, 115.7, 114.9, 114.6, 108.5 ($13 \times ArC$), 56.4 (OCH₃), 55.9 (OCH₃), 55.7 (OCH₃). HRMS (ESI): m/z calcd for $C_{25}H_{23}N_5O_6 + H^+$: 490.1727 [M + H] $^+$; found: 490.1720.

5.2.2.25 | 2-(2-(3-Chlorobenzylidene)Hydrazinyl)-4,6-Bis(4-Methoxyphenoxy)-1,3,5-Triazine (4j). Yield: 65%; mp: 236°C–238°C; R_f : 0.72. IR (ATR, $\bar{\nu}$): 3235 (NH), 3052 ($C_{sp2}-H_{stretch.}$), 2833 ($C_{sp3}-H_{stretch.}$), 1613 (C=N), 1578, 1504 ($2 \times C=C$), 1370, 1197 ($2 \times C-O_{stretch.}$) cm^{-1} . 1H NMR (300 MHz, DMSO- d_6): δ 11.91 (1H, s, NH), 8.13 (1H, s, H—C=N), 7.67 (1H, s, ArH), 7.56–7.53 (1H, m, ArH), 7.45–7.43 (2H, m, ArH), 7.21–7.14 (4H, m, ArH), 6.99–6.94 (4H, m, ArH), 3.77 (6H, s, $2 \times OCH_3$). ^{13}C NMR (75 MHz, DMSO- d_6): δ 173.1, 172.4, 167.0 ($3 \times C$ -triazine), 144.2 (H—C=N), 157.2, 145.6, 137.0, 134.0, 131.1, 129.9, 126.3, 126.1, 123.0, 114.9, 114.6 ($11 \times ArC$), 55.9 ($2 \times OCH_3$). HRMS (ESI): m/z calcd for $C_{24}H_{20}ClN_5O_4 + Na^+$: 500.1102 [M + Na] $^+$; found: 500.1097.

5.2.2.26 | 2-(2-(4-Chlorobenzylidene)Hydrazinyl)-4,6-Bis(4-Methoxyphenoxy)-1,3,5-Triazine (4k). Yield: 65%; mp: 224°C–226°C; R_f : 0.72. IR (ATR, $\bar{\nu}$): 3235 (NH stretch), 3060 ($C_{sp2}-H_{stretch.}$), 2834 ($C_{sp3}-H_{stretch.}$), 1613 (C=N), 1578, 1504 ($2 \times C=C$), 1370, 1197 ($2 \times C-O_{stretch.}$) cm^{-1} . 1H NMR (300 MHz, DMSO- d_6): δ 11.84 (1H, s, NH), 8.15 (1H, s, H—C=N), 7.65 (2H, d, $J = 8.4$ Hz, ArH), 7.47 (2H, d, $J = 8.4$ Hz, ArH), 7.20–7.13 (4H, m, ArH), 6.99–6.94 (4H, m, ArH), 3.77 (6H, s, $2 \times OCH_3$). ^{13}C NMR (75 MHz, DMSO- d_6): δ 173.1, 172.3, 167.0 ($3 \times C$ -triazine), 144.7 (H—C=N), 157.2, 145.6, 134.7, 133.7, 129.3, 128.9, 123.0, 114.9, 114.7 ($9 \times ArC$), 55.9 ($2 \times OCH_3$). HRMS (ESI): m/z calcd for $C_{24}H_{20}ClN_5O_4 + Na^+$: 500.1102 [M + Na] $^+$; found: 500.1093.

5.2.2.27 | 4,6-Bis(4-Methoxyphenoxy)-2-(2-(3-Nitrobenzylidene)-1,3,5-Triazine (4l). Yield: 68%; mp: 260°C–264°C; R_f : 0.58. IR (ATR, $\bar{\nu}$): 3229 (NH), 3058

($C_{sp2}-H_{stretch.}$), 2833 ($C_{sp3}-H_{stretch.}$), 1615 (C=N), 1583, 1505 ($2 \times C=C$), 1374, 1208 ($2 \times C-O_{stretch.}$) cm^{-1} . 1H NMR (300 MHz, DMSO- d_6): δ 12.03 (1H, s, NH), 8.46 (1H, s, ArH), 8.26–8.21 (2H, m, ArH, H—C=N), 8.02 (1H, d, $J = 7.5$ Hz, ArH), 7.70 (1H, t, $J = 7.8$ Hz, ArH), 7.23–7.15 (4H, m, ArH), 7.00–6.96 (4H, m, ArH), 3.77 (6H, s, $2 \times OCH_3$). ^{13}C NMR (75 MHz, DMSO- d_6): δ 173.0, 172.5, 167.1 ($3 \times C$ -triazine), 143.6 (H—C=N), 157.2, 148.6, 145.6, 136.6, 133.7, 130.8, 124.4, 123.0, 120.9, 114.9, 114.7 ($11 \times ArC$), 55.9 ($2 \times OCH_3$). HRMS (ESI): m/z calcd for $C_{24}H_{20}N_6O_6 + Na^+$: 511.1342 [M + Na] $^+$; found: 511.1333.

5.2.2.28 | 4,6-Bis(4-Methoxyphenoxy)-2-(2-(4-Nitrobenzylidene)-1,3,5-Triazine (4m). Yield: 68%; mp: 221°C–223°C; R_f : 0.56. IR (ATR, $\bar{\nu}$): 3301 (NH), 3058 ($C_{sp2}-H_{stretch.}$), 2838 ($C_{sp3}-H_{stretch.}$), 1615 (C=N), 1585, 1501 ($2 \times C=C$), 1367, 1199 ($2 \times C-O_{stretch.}$) cm^{-1} . 1H NMR (300 MHz, DMSO- d_6): δ 12.08 (1H, s, NH), 8.27–8.24 (3H, m, ArH, H—C=N), 7.89–7.87 (2H, d, $J = 8.7$ Hz, ArH), 7.21–7.12 (4H, m, ArH), 7.00–6.95 (4H, m, ArH), 3.78 (3H, s, OCH₃), 3.75 (3H, s, OCH₃). ^{13}C NMR (75 MHz, DMSO- d_6): δ 173.1, 172.4, 167.1 ($3 \times C$ -triazine), 141.0 (H—C=N), 157.2, 148.0, 145.6, 143.5, 128.1, 124.5, 123.0, 114.9, 114.7 ($9 \times ArC$), 55.9 ($2 \times OCH_3$). HRMS (ESI): m/z calcd for $C_{24}H_{20}N_6O_6 + Na^+$: 511.1342 [M + Na] $^+$; found: 511.1338.

5.2.2.29 | 4,6-Bis(4-Methoxyphenoxy)-2-(2-(Pyridin-3-Ylmethylene)Hydrazinyl)-1,3,5-Triazine (4n). Yield: 70%; mp: 210°C–212°C; R_f : 0.60. IR (ATR, $\bar{\nu}$): 3224 (NH), 3108 ($C_{sp2}-H_{stretch.}$), 2836 ($C_{sp3}-H_{stretch.}$), 1595 (C=N), 1577, 1504 ($2 \times C=C$), 1368, 1177 ($2 \times C-O_{stretch.}$) cm^{-1} . 1H NMR (300 MHz, DMSO- d_6): δ 11.95 (1H, s, NH), 8.75 (1H, d, $J = 1.8$ Hz, ArH), 8.57 (1H, dd, $J = 4.8, 1.8$ Hz, ArH), 8.19 (1H, s, H—C=N), 7.54 (1H, dt, $J = 7.8, 1.8$ Hz, ArH), 7.44 (1H, dd, $J = 7.8, 1.8$ Hz, ArH), 7.20–7.14 (4H, m, ArH), 6.99–6.94 (4H, m, ArH), 3.78 (3H, s, OCH₃), 3.76 (3H, s, OCH₃). ^{13}C NMR (75 MHz, DMSO- d_6): δ 173.1, 172.4, 167.0 ($3 \times C$ -triazine), 143.2 (H—C=N), 157.2, 150.9, 148.8, 145.6, 133.7, 130.6, 124.4, 123.0, 114.9, 114.7 ($10 \times ArC$), 55.9 ($2 \times OCH_3$). HRMS (ESI): m/z calcd for $C_{23}H_{20}N_6O_4 + H^+$: 445.1624 [M + H] $^+$; found: 445.1611.

5.2.2.30 | 4,6-Bis(4-Methoxyphenoxy)-2-(2-(Pyridin-4-Ylmethylene)Hydrazinyl)-1,3,5-Triazine (4o). Yield: 70%; mp: 226°C–228°C; R_f : 0.60. IR (ATR, $\bar{\nu}$): 3232 (NH), 3065 ($C_{sp2}-H_{stretch.}$), 2838 ($C_{sp3}-H_{stretch.}$), 1615 (C=N), 1563, 1499 ($2 \times C=C$), 1364, 1199 ($2 \times C-O_{stretch.}$) cm^{-1} . 1H NMR (300 MHz, DMSO- d_6): δ 12.06 (1H, s, NH), 8.60 (2H, d, $J = 4.8$ Hz, ArH), 8.13 (1H, s, H—C=N), 7.55 (2H, d, $J = 4.8$ Hz, ArH), 7.20–7.14 (4H, m, ArH), 7.00–6.97 (4H, m, ArH), 3.78 (3H, s, OCH₃), 3.76 (3H, s, OCH₃). ^{13}C NMR (75 MHz, DMSO- d_6): δ 173.1, 172.4, 167.1 ($3 \times C$ -triazine), 141.9 (H—C=N), 157.2, 150.5, 145.6, 143.4, 123.0, 121.2, 114.9, 114.7 ($8 \times ArC$), 55.9 ($2 \times OCH_3$). HRMS (ESI): m/z calcd for $C_{23}H_{20}N_6O_4 + H^+$: 445.1624 [M + H] $^+$; found: 445.1617.

5.2.2.31 | 2-(2-Benzylidenehydrazinyl)-4,6-Bis(4-Methylphenoxy)-1,3,5-Triazine (5a). Yield: 70%; mp: 218°C–219°C; R_f : 0.70. IR (ATR, $\bar{\nu}$): 3243 (NH), 3030 ($C_{sp2}-H_{stretch.}$), 2918 ($C_{sp3}-H_{stretch.}$), 1604 (C=N), 1570, 1504 ($2 \times C=C$), 1359, 1199 ($2 \times C-O_{stretch.}$) cm^{-1} . 1H NMR (300 MHz, DMSO- d_6): δ 11.79 (1H, s, NH), 8.16 (1H, s, H—C=N), 7.62 (2H, m, ArH), 7.43–7.40 (3H, m, ArH), 7.26–7.20 (4H, m, ArH), 6.71–7.08 (4H, m, ArH), 2.34 (3H, s, OCH₃), 2.31 (3H, s, OCH₃). ^{13}C NMR

(75 MHz, DMSO- d_6): δ 172.9, 172.1, 166.9 (3 \times C-triazine), 146.2 (H—C=N), 150.0, 135.3, 135.1, 134.7, 130.4, 130.1, 129.2, 127.3, 121.9 (9 \times ArC), 20.8 (2 \times CH₃). HRMS (ESI): m/z calcd for C₂₄H₂₁N₅O₂ + H⁺: 412.1773 [M + H]⁺; found: 412.1765.

5.2.2.32 | 2-(2-(2-Hydroxybenzylidene)Hydrazinyl)-4,6-Bis(4-Methylphenoxy)-1,3,5-Triazine (5b). Yield: 78%; mp: 260°C–262°C; R_f : 0.60. IR (ATR, $\bar{\nu}$): 3350–2500 (br., OH), 3232 (NH), 3087 (C_{sp2}—H_{stretch.}), 2921 (C_{sp3}—H_{stretch.}), 1620 (C=N), 1575, 1504 (2 \times C=C), 1370, 1194 (2 \times C—O_{stretch.}) cm^{−1}. ¹H NMR (300 MHz, DMSO- d_6): δ 12.06 (1H, s, NH), 10.93 (1H, s, OH), 8.32 (1H, s, H—C=N), 7.40 (1H, dd, J = 7.8, 1.5 Hz, ArH), 7.29–7.21 (5H, m, ArH), 7.15–7.09 (4H, m, ArH), 6.90–6.88 (2H, m, ArH), 2.35 (3H, s, CH₃), 2.31 (3H, s, CH₃). ¹³C NMR (75 MHz, DMSO- d_6): δ 172.9, 172.3, 166.4 (3 \times C-triazine), 147.0 (H—C=N), 149.9, 135.4, 135.2, 131.6, 130.4, 130.2, 130.0, 121.9, 121.8, 119.7, 118.9, 116.9 (12 \times ArC), 20.9 (CH₃), 20.8 (CH₃). HRMS (ESI): m/z calcd for C₂₄H₂₁N₅O₃ + H⁺: 428.1723 [M + H]⁺; found: 428.1715.

5.2.2.33 | 2-(2-(3-Hydroxybenzylidenehydrazinyl)-4,6-Bis(4-Methylphenoxy)-1,3,5-Triazine (5c). Yield: 68%; mp: 274°C–276°C; R_f : 0.53. IR (ATR, $\bar{\nu}$): 3500–2500 (br., OH), 3231 (NH), 3032 (C_{sp2}—H_{stretch.}), 2918 (C_{sp3}—H_{stretch.}), 1613 (C=N), 1575, 1503 (2 \times C=C), 1369, 1193 (2 \times C—O_{stretch.}) cm^{−1}. ¹H NMR (300 MHz, DMSO- d_6): δ 11.74 (1H, s, NH), 9.61 (1H, s, OH), 8.08 (1H, s, H—C=N), 7.25–7.08 (10H, m, ArH), 6.99 (1H, d, J = 7.5 Hz, ArH), 6.80 (1H, m, ArH), 2.35 (3H, s, CH₃), 2.31 (3H, s, CH₃). ¹³C NMR (75 MHz, DMSO- d_6): δ 173.0, 172.1, 166.9 (3 \times C-triazine), 146.4 (H—C=N), 158.1, 150.0, 136.0, 135.3, 135.1, 130.4, 130.2, 130.1, 121.9, 119.0, 117.7, 112.9 (12 \times ArC), 20.8 (2 \times CH₃). HRMS (ESI): m/z calcd for C₂₄H₂₁N₅O₃ + H⁺: 428.1723 [M + H]⁺; found: 428.1719.

5.2.2.34 | 2-(2-(4-Hydroxybenzylidenehydrazinyl)-4,6-Bis(4-Methylphenoxy)-1,3,5-Triazine (5d). Yield: 67%; mp: 212°C–214°C; R_f : 0.50. IR (ATR, $\bar{\nu}$): 3500–2500 (br., OH), 3231 (NH), 3088 (C_{sp2}—H_{stretch.}), 2920 (C_{sp3}—H_{stretch.}), 1607 (C=N), 1571, 1505 (2 \times C=C), 1370, 1198 (2 \times C—O_{stretch.}) cm^{−1}. ¹H NMR (300 MHz, DMSO- d_6): δ 11.59 (1H, s, NH), 9.91 (1H, s, OH), 8.06 (1H, s, H—C=N), 7.45 (2H, d, J = 8.7 Hz, ArH), 7.25–7.19 (4H, m, ArH), 7.15–7.07 (4H, m, ArH), 6.79 (2H, d, J = 8.4 Hz, ArH), 2.34 (3H, s, CH₃), 2.30 (3H, s, CH₃). ¹³C NMR (75 MHz, DMSO- d_6): δ 172.9, 172.0, 166.6 (3 \times C-triazine), 146.6 (H—C=N), 159.7, 150.1, 135.2, 135.1, 130.4, 130.1, 129.1, 125.7, 121.9, 121.8, 116.1 (11 \times ArC), 20.8 (2 \times CH₃). HRMS (ESI): m/z calcd for C₂₄H₂₁N₅O₃ + H⁺: 428.1723 [M + H]⁺; found: 428.1709.

5.2.2.35 | 2-(2-(4-Methoxybenzylidene)Hydrazinyl)-4,6-Bis(4-Methylphenoxy)-1,3,5-Triazine (5e). Yield: 70%; m.p: 210°C–212°C; R_f : 0.67. IR (ATR, $\bar{\nu}$): 3235 (NH), 3034 (C_{sp2}—H_{stretch.}), 2923 (C_{sp3}—H_{stretch.}), 1602 (C=N), 1573, 1508 (2 \times C=C), 1369, 1218 (2 \times C—O_{stretch.}) cm^{−1}. ¹H NMR (300 MHz, DMSO- d_6): δ 11.67 (1H, s, NH), 8.11 (1H, s, H—C=N), 7.56 (2H, d, J = 8.7 Hz, ArH), 7.25–7.08 (8H, m, ArH), 6.97 (2H, d, J = 8.7 Hz, ArH), 3.79 (3H, s, OCH₃), 2.34 (3H, s, CH₃), 2.31 (3H, s, CH₃). ¹³C NMR (75 MHz, DMSO- d_6): δ 172.9, 172.0, 166.7 (3 \times C-triazine), 146.2 (H—C=N), 161.1, 150.1, 135.2, 135.1, 130.4, 130.1, 128.9, 127.3, 121.9, 114.7 (10 \times ArC), 55.7 (OCH₃), 20.8 (2 \times CH₃). HRMS (ESI): m/z calcd for C₂₅H₂₃N₅O₃ + H⁺: 442.1879 [M + H]⁺; found: 442.1871.

5.2.2.36 | 2-(2-(4-Methylbenzylidene)Hydrazinyl)-4,6-Bis(4-Methylphenoxy)-1,3,5-Triazine (5f). Yield: 65%; mp: 209°C–211°C; R_f : 0.77. IR (ATR, $\bar{\nu}$): 3237 (NH), 3036 (C_{sp2}—H_{stretch.}), 2918 (C_{sp3}—H_{stretch.}), 1597 (C=N), 1574, 1509 (2 \times C=C), 1370, 1200 (2 \times C—O_{stretch.}) cm^{−1}. ¹H NMR (300 MHz, DMSO- d_6): δ 11.73 (1H, s, NH), 8.13 (1H, s, H—C=N), 7.51 (2H, d, J = 7.8 Hz, ArH), 7.24–7.08 (10H, m, ArH), 2.34 (3H, s, CH₃), 2.33 (3H, s, CH₃), 2.31 (3H, s, CH₃). ¹³C NMR (75 MHz, DMSO- d_6): δ 172.9, 172.1, 166.8 (3 \times C-triazine), 146.3 (H—C=N), 150.0, 140.1, 135.3, 135.1, 132.0, 130.4, 130.1, 129.8, 127.3, 121.9 (10 \times ArC), 21.4 (2 \times CH₃), 20.8 (CH₃). HRMS (ESI): m/z calcd for C₂₅H₂₃N₅O₂ + H⁺: 426.1930 [M + H]⁺; found: 426.1918.

5.2.2.37 | 2-(2-(4-*N,N*-Dimethylaminobenzylidene)Hydrazinyl)-4,6-Bis(4-Methylphenoxy)-1,3,5-Triazine (5g). Yield: 73%; mp: 216°C–218°C; R_f : 0.65. IR (ATR, $\bar{\nu}$): 3247 (NH), 3033 (C_{sp2}—H_{stretch.}), 2916 (C_{sp3}—H_{stretch.}), 1597 (C=N), 1568, 1503 (2 \times C=C), 1364, 1199 (2 \times C—O_{stretch.}) cm^{−1}. ¹H NMR (300 MHz, CDCl₃): δ 8.56 (1H, s, NH), 7.71 (1H, s, H—C=N), 7.58 (2H, d, J = 9.0 Hz, ArH), 7.19–7.01 (8H, m, ArH), 6.66 (2H, d, J = 9.0 Hz, ArH), 3.02 (6H, s, N(CH₃)₂), 2.36 (6H, s, 2 \times CH₃). ¹³C NMR (75 MHz, CDCl₃): δ 173.2, 172.0, 166.0 (3 \times C-triazine), 147.2 (H—C=N), 151.7, 149.7, 135.3, 135.1, 129.8, 129.2, 121.4, 120.9, 111.5 (9 \times ArC), 40.1, 20.9 (2 \times CH₃). HRMS (ESI): m/z calcd for C₂₆H₂₆N₆O₂ + H⁺: 455.2195 [M + H]⁺; found: 455.2188.

5.2.2.38 | 2-((*E*)-3-Phenylallylidene)Hydrazinyl)-4,6-Bis(4-Methylphenoxy)-1,3,5-Triazine (5h). Yield: 77%; mp: 225°C–227°C; R_f : 0.69. IR (ATR, $\bar{\nu}$): 3235 (NH), 3054 (C_{sp2}—H_{stretch.}), 2916 (C_{sp3}—H_{stretch.}), 1625 (C=N), 1567, 1503 (2 \times C=C), 1366, 1193 (2 \times C—O_{stretch.}) cm^{−1}. ¹H NMR (300 MHz, DMSO- d_6): δ 11.67 (1H, s, NH), 7.98 (1H, dd, J = 6.6, 1.8 Hz, H—C=N), 7.59 (2H, d, J = 6.9 Hz, ArH), 7.40–7.30 (3H, m, ArH), 7.24–7.20 (4H, m, ArH), 7.13–7.08 (4H, m, ArH), 6.91–7.30 (2H, m, (CH=CHAr)), 2.32 (3H, s, CH₃), 2.31 (3H, s, CH₃). ¹³C NMR (75 MHz, DMSO- d_6): δ 172.9, 172.1, 166.7 (3 \times C-triazine), 148.8 (H—C=N), 150.0, 139.2, 135.3, 135.1, 130.4, 130.3, 129.2, 127.5 (8 \times ArC), 136.3 ((CH=CHAr)), 125.8 (CH=CHAr), 121.87, 20.8 (2 \times CH₃). HRMS (ESI): m/z calcd for C₂₆H₂₃N₅O₂ + Na⁺: 460.1749 [M + Na]⁺; found: 460.1738.

5.2.2.39 | 2-(2-(4-Hydroxy-3-Methoxybenzylidene)Hydrazinyl)-4,6-Bis(4-Methyl-Phenoxy)-1,3,5-Triazine (5i). Yield: 60%; mp: 246°C–248°C; R_f : 0.60. IR (ATR, $\bar{\nu}$): 3497 (br., OH), 3237 (N—H), 3105 (C_{sp2}—H_{stretch.}), 2920 (C_{sp3}—H_{stretch.}), 1606 (C=N), 1573, 1506 (2 \times C=C), 1362, 1203 (2 \times C—O_{stretch.}) cm^{−1}. ¹H NMR (300 MHz, DMSO- d_6): δ 11.63 (1H, bs, NH), 9.52 (1H, bs, OH), 8.03 (1H, s, H—C=N), 7.24–7.08 (9H, m, ArH), 6.94 (1H, dd, J = 8.1, 1.5 Hz, ArH), 6.79 (1H, d, J = 8.1, ArH), 3.77 (3H, s, OCH₃), 2.31 (6H, s, 2 \times CH₃). ¹³C NMR (75 MHz, DMSO- d_6): δ 173.8, 172.1, 166.5 (3 \times C-triazine), 146.6 (H—C=N), 150.0, 149.2, 148.4, 135.2, 135.0, 130.4, 130.0, 126.1, 122.5, 122.0, 121.9, 115.7, 108.7 (13 \times ArC), 55.7 (OCH₃), 20.85 (CH₃). HRMS (ESI): m/z calcd for C₂₅H₂₃N₅O₄ + H⁺: 458.1828 [M + H]⁺; found: 458.1815.

5.2.2.40 | 2-(2-(3-Chlorobenzylidene)Hydrazinyl)-4,6-Bis(4-Methylphenoxy)-1,3,5-Triazine (5j). Yield: 70%; mp: 234°C–236°C; R_f : 0.71. IR (ATR, $\bar{\nu}$): 3238 (NH), 3039 (C_{sp2}—H_{stretch.}), 2919 (C_{sp3}—H_{stretch.}), 1609 (C=N), 1576, 1509 (2 \times C=C), 1370, 1202 (2 \times C—O_{stretch.}) cm^{−1}. ¹H NMR (300 MHz, CDCl₃): δ 9.21 (1H, s, NH), 7.89 (1H, s, H—C=N), 7.67 (1H, t,

$J = 1.5$ Hz, ArH), 7.46 (1H, td, $J = 7.2, 1.5$ Hz, ArH), 7.36–7.25 (2H, m, ArH), 7.20–7.05 (8H, m, ArH), 2.37 (6H, s, $2 \times \text{CH}_3$). ^{13}C NMR (75 MHz, DMSO- d_6): δ 172.9, 172.3, 167.0 ($3 \times \text{C-triazine}$), 144.1 (H-C=N), 150.0, 137.0, 135.3, 135.2, 134.0, 131.1, 130.4, 130.1, 129.9, 126.4, 126.0, 122.0, 121.9 ($12 \times \text{ArC}$), 20.8 ($2 \times \text{CH}_3$). HRMS (ESI): m/z calcd for $\text{C}_{24}\text{H}_{20}\text{ClN}_5\text{O}_2 + \text{Na}^+$: 468.1203 [$\text{M} + \text{Na}$] $^+$; found: 468.1195.

5.2.2.41 | 2-(2-(4-Chlorobenzylidene)Hydrazinyl)-4,6-Bis(4-Methylphenoxy)-1,3,5-Triazine (5k). Yield: 65%; mp: 238°C – 241°C ; R_f : 0.69. IR (ATR, $\bar{\nu}$): 3231 (NH), 3037 ($\text{C}_{\text{sp}2}\text{-H}_{\text{stretch.}}$), 2920 ($\text{C}_{\text{sp}3}\text{-H}_{\text{stretch.}}$), 1601 (C=N), 1575, 1509 ($2 \times \text{C=C}$), 1369, 1201 ($2 \times \text{C-O}_{\text{stretch.}}$) cm^{-1} . ^1H NMR (300 MHz, DMSO- d_6): δ 11.86 (1H, s, NH), 8.15 (1H, s, H-C=N), 7.64 (2H, d, $J = 8.4$ Hz, ArH), 7.48 (2H, d, $J = 8.4$ Hz, ArH), 7.25–7.08 (8H, m, ArH), 2.34 (3H, s, CH_3), 2.31 (3H, s, CH_3). ^{13}C NMR (75 MHz, DMSO- d_6): δ 172.9, 172.2, 167.9 ($3 \times \text{C-triazine}$), 144.8 (H-C=N), 150.0, 135.3, 135.2, 134.7, 133.7, 130.4, 130.1, 129.3, 128.9, 121.9 ($10 \times \text{ArC}$), 20.8 ($2 \times \text{CH}_3$). HRMS (ESI): m/z calcd for $\text{C}_{24}\text{H}_{20}\text{ClN}_5\text{O}_2 + \text{Na}^+$: 468.1203 [$\text{M} + \text{Na}$] $^+$; found: 468.1190.

5.2.2.42 | 2-(2-(3-Nitrobenzylidene)Hydrazinyl)-4,6-Bis(4-Methylphenoxy)-1,3,5-Triazine (5l). Yield: 60%; mp: 244°C – 246°C ; R_f : 0.75. IR (ATR, $\bar{\nu}$): 3232 (NH), 3037 ($\text{C}_{\text{sp}2}\text{-H}_{\text{stretch.}}$), 2922 ($\text{C}_{\text{sp}3}\text{-H}_{\text{stretch.}}$), 1613 (C=N), 1580, 1509 ($2 \times \text{C=C}$), 1376, 1203 ($2 \times \text{C-O}_{\text{stretch.}}$) cm^{-1} . ^1H NMR (300 MHz, DMSO- d_6): δ 12.04 (1H, s, NH), 8.43 (1H, s, ArH), 8.25 (1H, s, H-C=N), 8.21 (1H, dd, $J = 8.1, 2.1$ Hz, ArH), 8.00 (1H, d, $J = 7.8$ Hz, ArH), 7.69 (1H, t, $J = 7.8$ Hz, ArH), 7.20–7.10 (8H, m, ArH), 2.34 (3H, s, CH_3), 2.31 (3H, s, CH_3). ^{13}C NMR (75 MHz, DMSO- d_6): δ 172.9, 172.3, 167.0 ($3 \times \text{C-triazine}$), 143.6 (H-C=N), 150.0, 148.6, 136.5, 135.3, 135.2, 133.8, 130.8, 130.4, 130.1, 124.4, 121.9, 120.7 ($10 \times \text{ArC}$), 20.8 ($2 \times \text{CH}_3$). HRMS (ESI): m/z calcd for $\text{C}_{24}\text{H}_{20}\text{N}_6\text{O}_4 + \text{Na}^+$: 479.1444 [$\text{M} + \text{Na}$] $^+$; found: 479.1434.

5.2.2.43 | 2-(2-(4-Nitrobenzylidene)Hydrazinyl)-4,6-Bis(4-Methylphenoxy)-1,3,5-Triazine (5m). Yield: 70%; mp: 240°C – 243°C ; R_f : 0.65. IR (ATR, $\bar{\nu}$): 3229 (NH), 3040 ($\text{C}_{\text{sp}2}\text{-H}_{\text{stretch.}}$), 2918 ($\text{C}_{\text{sp}3}\text{-H}_{\text{stretch.}}$), 1610 (C=N), 1579, 1508 ($2 \times \text{C=C}$), 1346, 1201 ($2 \times \text{C-O}_{\text{stretch.}}$) cm^{-1} . ^1H NMR (300 MHz, DMSO- d_6): δ 12.09 (1H, s, NH), 8.26 (3H, m, H-C=N), 7.87 (2H, d, $J = 8.7$ Hz, ArH), 7.24–7.09 (8H, m, ArH), 2.34 (3H, s, CH_3), 2.32 (3H, s, CH_3). ^{13}C NMR (75 MHz, DMSO- d_6): δ 173.0, 172.3, 167.1 ($3 \times \text{C-triazine}$), 143.5 (H-C=N), 150.0, 148.0, 141.0, 135.3, 130.4, 130.2, 128.1, 124.5, 121.9 ($9 \times \text{ArC}$), 20.8 ($2 \times \text{CH}_3$). HRMS (ESI): m/z calcd for $\text{C}_{24}\text{H}_{20}\text{N}_6\text{O}_4 + \text{Na}^+$: 479.1444 [$\text{M} + \text{Na}$] $^+$; found: 479.1430.

5.2.2.44 | 2-(2-(Pyridin-3-Ylmethylene)Hydrazinyl)-4,6-Bis(4-Methylphenoxy)-1,3,5-Triazine (5n). Yield: 75%; mp: 213°C – 215°C ; R_f : 0.70. IR (ATR, $\bar{\nu}$): 3232 (NH), 3037 ($\text{C}_{\text{sp}2}\text{-H}_{\text{stretch.}}$), 2921 ($\text{C}_{\text{sp}3}\text{-H}_{\text{stretch.}}$), 1599 (C=N), 1578, 1508 ($2 \times \text{C=C}$), 1370, 1202 ($2 \times \text{C-O}_{\text{stretch.}}$) cm^{-1} . ^1H NMR (300 MHz, DMSO- d_6): δ 11.95 (1H, s, NH), 8.74 (1H, d, $J = 1.8$ Hz, ArH), 8.57 (1H, dd, $J = 6.3, 1.5$ Hz, ArH), 8.19 (1H, s, H-C=N), 8.01 (1H, td, $J = 7.8, 2.1$ Hz, ArH), 7.44 (1H, dd, $J = 8.1, 4.8$ Hz, ArH), 7.25–7.09 (8H, m, ArH), 2.33 (3H, s, CH_3), 2.31 (3H, s, CH_3). ^{13}C NMR (75 MHz, DMSO- d_6): δ 173.0, 172.2, 167.0 ($3 \times \text{C-triazine}$), 143.3 (H-C=N), 150.9, 150.0, 148.8, 135.3, 133.7, 130.6, 130.4, 130.1, 124.4, 121.9 ($10 \times \text{ArC}$), 20.8 ($2 \times \text{CH}_3$). HRMS (ESI): m/z calcd for $\text{C}_{23}\text{H}_{20}\text{N}_6\text{O}_2 + \text{H}^+$: 413.1726 [$\text{M} + \text{H}$] $^+$; found: 413.1711.

5.2.2.45 | 2-(2-(Pyridin-4-Ylmethylene)Hydrazinyl)-4,6-Bis(4-Methylphenoxy)-1,3,5-Triazine (5o). Yield: 75%; mp: 207°C – 208°C ; R_f : 0.70. IR (ATR, $\bar{\nu}$): 3234 (NH), 3035 ($\text{C}_{\text{sp}2}\text{-H}_{\text{stretch.}}$), 2916 ($\text{C}_{\text{sp}3}\text{-H}_{\text{stretch.}}$), 1617 (C=N), 1573, 1505 ($2 \times \text{C=C}$), 1375, 1201 ($2 \times \text{C-O}_{\text{stretch.}}$) cm^{-1} . ^1H NMR (300 MHz, DMSO- d_6): δ 12.06 (1H, s, NH), 8.61–8.60 (2H, d, $J = 4.8$ Hz, ArH), 8.13 (1H, s, H-C=N), 7.55 (2H, d, $J = 6.0$ Hz, ArH), 7.25–7.10 (8H, m, ArH), 2.33 (3H, s, CH_3), 3.31 (3H, s, CH_3). ^{13}C NMR (75 MHz, DMSO- d_6): δ 173.0, 172.3, 167.1 ($3 \times \text{C-triazine}$), 143.5 (H-C=N), 150.6, 150.0, 141.9, 135.3, 130.4, 130.1, 121.9, 121.2 ($8 \times \text{ArC}$), 20.8 ($2 \times \text{CH}_3$). HRMS (ESI): m/z calcd for $\text{C}_{23}\text{H}_{20}\text{N}_6\text{O}_2 + \text{H}^+$: 413.1726 [$\text{M} + \text{H}$] $^+$; found: 413.1709.

5.2.2.46 | 2-(2-Benzylidenehydrazinyl)-4,6-Bis(4-Chlorophenoxy)-1,3,5-Triazine (6a). Yield: 75%; mp: 227°C – 228°C ; R_f : 0.70. IR (ATR, $\bar{\nu}$): 3235 (NH), 3062 ($\text{C}_{\text{sp}2}\text{-H}_{\text{stretch.}}$), 1608 (C=N), 1572, 1488 ($2 \times \text{C=C}$), 1366, 1215 ($2 \times \text{C-O}_{\text{stretch.}}$), 1085 ($\text{C-Cl}_{\text{stretch.}}$) cm^{-1} . ^1H NMR (300 MHz, CDCl_3): δ 9.00 (1H, s, NH), 8.16 (1H, s, H-C=N), 7.70–7.67 (2H, m, ArH), 7.43–7.38 (7H, m, ArH), 7.18–7.07 (4H, m, ArH). ^{13}C NMR (75 MHz, CDCl_3): δ 172.8, 171.8, 166.5 ($3 \times \text{C-triazine}$), 146.8 (H-C=N), 150.1, 133.2, 130.6, 130.1, 129.5, 128.7, 127.7, 123.1 ($8 \times \text{ArC}$). HRMS (ESI): m/z calcd for $\text{C}_{22}\text{H}_{15}\text{Cl}_2\text{N}_5\text{O}_2 + \text{H}^+$: 452.0681 [$\text{M} + \text{H}$] $^+$; found: 452.0670.

5.2.2.47 | 2-(2-(2-Hydroxybenzylidene)Hydrazinyl)-4,6-Bis(4-Chlorophenoxy)-1,3,5-Triazine (6b). Yield: 78%; mp: 257°C – 259°C ; R_f : 0.60. IR (ATR, $\bar{\nu}$): 3300–2800 (br., OH), 3226 (NH), 3062 ($\text{C}_{\text{sp}2}\text{-H}_{\text{stretch.}}$), 1618 (C=N), 1574, 1485 ($2 \times \text{C=C}$), 1369, 1202 ($2 \times \text{C-O}_{\text{stretch.}}$), 1085 ($\text{C-Cl}_{\text{stretch.}}$) cm^{-1} . ^1H NMR (300 MHz, CDCl_3): δ 10.68 (1H, s, NH), 10.13 (1H, s, OH), 8.19 (1H, s, H-C=N), 7.42–7.38 (4H, m, ArH), 7.30–7.24 (1H, m, ArH), 7.17–7.12 (4H, m, ArH), 6.97 (1H, d, $J = 8.4$ Hz, ArH), 6.87–6.84 (1H, m, ArH), 6.79–6.76 (1H, m, ArH). ^{13}C NMR (75 MHz, DMSO- d_6): δ 172.6, 172.1, 166.4 ($3 \times \text{C-triazine}$), 147.3 (H-C=N), 157.8, 151.0, 150.9, 131.7, 130.4, 130.3, 130.1, 130.0, 129.8, 124.2, 124.1, 119.7, 118.9, 116.9 ($14 \times \text{ArC}$). HRMS (ESI): m/z calcd for $\text{C}_{22}\text{H}_{15}\text{Cl}_2\text{N}_5\text{O}_3 + \text{H}^+$: 468.0630 [$\text{M} + \text{H}$] $^+$; found: 468.0622.

5.2.2.48 | 2-(2-(3-Hydroxybenzylidene)Hydrazinyl)-4,6-Bis(4-Chlorophenoxy)-1,3,5-Triazine (6c). Yield: 70%; mp: 270°C – 272°C ; R_f : 0.65. IR (ATR, $\bar{\nu}$): 3500–2900 (br., OH), 3226 (NH), 3059 ($\text{C}_{\text{sp}2}\text{-H}_{\text{stretch.}}$), 1608 (C=N), 1568, 1483 ($2 \times \text{C=C}$), 1370, 1199 ($2 \times \text{C-O}_{\text{stretch.}}$), 1085 ($\text{C-Cl}_{\text{stretch.}}$) cm^{-1} . ^1H NMR (300 MHz, DMSO- d_6): δ 11.82 (1H, s, NH), 9.62 (1H, s, OH), 8.09 (1H, s, H-C=N), 7.52–7.47 (4H, m, ArH), 7.33–7.19 (5H, m, ArH), 7.13 (1H, t, $J = 1.5$ Hz, ArH), 7.00 (1H, d, $J = 7.8$ Hz, ArH), 6.80 (1H, dd, $J = 7.8, 2.1$ Hz, ArH). ^{13}C NMR (75 MHz, DMSO- d_6): δ 172.6, 171.8, 166.9 ($3 \times \text{C-triazine}$), 146.8 (H-C=N), 158.1, 151.0, 135.9, 130.3, 130.2, 129.9, 129.7, 124.2, 119.0, 117.8, 113.0 ($11 \times \text{ArC}$). HRMS (ESI): m/z calcd for $\text{C}_{22}\text{H}_{15}\text{Cl}_2\text{N}_5\text{O}_3 + \text{H}^+$: 468.0630 [$\text{M} + \text{H}$] $^+$; found: 468.0608.

5.2.2.49 | 2-(2-(4-Hydroxybenzylidene)Hydrazinyl)-4,6-Bis(4-Chlorophenoxy)-1,3,5-Triazine (6d). Yield: 80%; mp: 194°C ; R_f : 0.66. IR (ATR, $\bar{\nu}$): 3500–2500 (br., OH), 3233 (NH), 3130 ($\text{C}_{\text{sp}2}\text{-H}_{\text{stretch.}}$), 1603 (C=N), 1569, 1484 ($2 \times \text{C=C}$), 1370, 1202 ($2 \times \text{C-O}_{\text{stretch.}}$), 1085 ($\text{C-Cl}_{\text{stretch.}}$) cm^{-1} . ^1H NMR (300 MHz, DMSO- d_6): δ 11.67 (1H, s, NH), 9.99 (1H, s, OH), 8.05 (1H, s, H-C=N), 7.52–7.43 (6H, m, ArH), 7.32–7.26 (4H, m, ArH), 6.79 (2H, d, $J = 8.7$ Hz, ArH). ^{13}C NMR (75 MHz, DMSO- d_6): δ 172.6,

171.8, 166.6 (3 × C-triazine), 146.9 (H—C=N), 159.8, 151.0, 130.3, 130.2, 129.9, 129.6, 129.2, 125.7, 124.3, 116.1 (10 × ArC). HRMS (ESI): *m/z* calcd for C₂₂H₁₅Cl₂N₅O₃ + H⁺: 468.0630 [M + H]⁺; found: 468.0628.

5.2.2.50 | 4,6-Bis(4-Chlorophenoxy)-2-(2-(4-Methoxybenzylidene)Hydrazinyl)-1,3,5-Triazine (6e). Yield: 70%; mp: 260°C–262°C; *R*_f: 0.68. IR (ATR, $\bar{\nu}$): 3253 (NH), 3059 (C_{sp2}—H_{stretch.}), 2998 (C_{sp3}—H_{stretch.}), 1608 (C=N), 1568, 1485 (2 × C=C), 1371, 1217 (2 × C—O_{stretch.}), 1084 (C—Cl_{stretch.}) cm^{−1}. ¹H NMR (300 MHz, DMSO-*d*₆): δ 11.76 (1H, s, NH), 8.11 (1H, s, H—C=N), 7.57 (2H, d, *J* = 8.7 Hz, ArH), 7.52–7.47 (4H, m, ArH), 7.33–7.26 (4H, m, ArH), 6.98 (2H, d, *J* = 8.7 Hz, ArH), 3.79 (3H, s, OCH₃). ¹³C NMR (75 MHz, DMSO-*d*₆): δ 172.6, 171.8, 166.7 (3 × C-triazine), 146.5 (H—C=N), 161.2, 150.0, 130.3, 130.2, 129.9, 129.7, 129.0, 127.2, 124.2, 114.7 (10 × ArC), 55.7 (OCH₃). HRMS (ESI): *m/z* calcd for C₂₃H₁₇Cl₂N₅O₃ + Na⁺: 504.0606 [M + Na]⁺; found: 504.0596.

5.2.2.51 | 4,6-Bis(4-Chlorophenoxy)-2-(2-(4-Methylbenzylidene)Hydrazinyl)-1,3,5-Triazine (6f). Yield: 85%; mp: 238°C–239°C; *R*_f: 0.72. IR (ATR, $\bar{\nu}$): 3223 (NH), 3066 (C_{sp2}—H_{stretch.}), 3001 (C_{sp3}—H_{stretch.}), 1619 (C=N), 1574, 1485 (2 × C=C_{stretch.}), 1372, 1205 (2 × C—O_{stretch.}), 1083 (C—Cl_{stretch.}) cm^{−1}. ¹H NMR (300 MHz, DMSO-*d*₆): δ 11.82 (1H, s, NH), 8.13 (1H, s, H—C=N), 7.53–7.47 (6H, m, ArH), 7.33–7.22 (6H, m, ArH), 2.33 (3H, s, CH₃). ¹³C NMR (75 MHz, DMSO-*d*₆): δ 172.6, 171.8, 166.8 (3 × C-triazine), 146.6 (H—C=N), 151.0, 140.4, 132.0, 130.3, 130.2, 129.9, 129.8, 129.7, 127.4, 124.2 (10 × ArC), 21.5 (CH₃). HRMS (ESI): *m/z* calcd for C₂₃H₁₇Cl₂N₅O₂ + H⁺: 466.0838 [M + H]⁺; found: 466.0822.

5.2.2.52 | 2-(2-(4-*N,N*-Dimethylaminobenzylidene)Hydrazinyl)-4,6-Bis(4-Chlorophenoxy)-1,3,5-Triazine (6g). Yield: 93%; mp: 226°C–228°C; *R*_f: 0.80. IR (ATR, $\bar{\nu}$): 3243 (NH), 3030 (C_{sp2}—H_{stretch.}), 2895 (C_{sp3}—H_{stretch.}), 1599 (C=N), 1572, 1483 (2 × C=C), 1366, 1193 (2 × C—O_{stretch.}), 1084 (C—Cl_{stretch.}) cm^{−1}. ¹H NMR (300 MHz, DMSO-*d*₆): δ 11.56 (1H, s, NH), 8.03 (1H, s, H—C=N), 7.50–7.42 (6H, m, ArH), 7.31–7.24 (4H, m, ArH), 6.71 (2H, d, *J* = 8.7 Hz, ArH), 2.95 (6H, s, N(CH₃)₂). ¹³C NMR (75 MHz, DMSO-*d*₆): δ 172.6, 171.6, 166.3 (3 × C-triazine), 147.7 (H—C=N), 151.9, 151.0, 130.3, 130.1, 129.9, 129.7, 128.8, 124.2, 121.8, 112.2 (10 × ArC), 39.4 N(CH₃)₂. HRMS (ESI): *m/z* calcd for C₂₄H₂₀Cl₂N₆O₂ + H⁺: 495.1103 [M + H]⁺; found: 495.1098.

5.2.2.53 | 6-Bis(4-Chlorophenoxy)-2-(2-((*E*)-3-Phenylallylidene)Hydrazinyl)-1,3,5-Triazine (6h). Yield: 87%; mp: 248°C–250°C; *R*_f: 0.73. IR (ATR, $\bar{\nu}$): 3240 (NH), 3039 (C_{sp2}—H_{stretch.}), 1626 (C=N), 1574, 1485 (2 × C=C), 1366, 1209 (2 × C—O_{stretch.}), 1085 (C—Cl_{stretch.}) cm^{−1}. ¹H NMR (300 MHz, DMSO-*d*₆): δ 11.76 (1H, s, NH), 7.99 (1H, dd, *J* = 5.1, 3.0 Hz, H—C=N), 7.61–7.47 (6H, m, ArH), 7.39–7.26 (7H, m, ArH), 6.99–6.97 (2H, m, (CH=CHAr)). ¹³C NMR (75 MHz, DMSO-*d*₆): δ 172.6, 171.8, 166.6 (3 × C-triazine), 149.2 (H—C=N), 139.5, 151.0, 130.4, 130.2, 130.0, 129.8, 129.3, 127.6, 124.2, 124.1 (10 × ArC), 136.3 (CH=CHAr), 125.7 (CH=CHAr). HRMS (ESI): *m/z* calcd for C₂₄H₁₇Cl₂N₅O₂ + H⁺: 478.0838 [M + H]⁺; found: 478.0825.

5.2.2.54 | 2-(2-(4-Hydroxy-3-Methoxybenzylidene)Hydrazinyl)-4,6-Bis(4-Chlorophenoxy)-1,3,5-Triazine (6i).

Yield: 85%; mp: 218°C–220°C; *R*_f: 0.80. IR (ATR, $\bar{\nu}$): 3417 (br., OH), 3232 (NH), 3060 (C_{sp2}—H_{stretch.}), 2945 (C_{sp3}—H_{stretch.}), 1608 (C=N), 1575, 1488 (2 × C=C), 1367, 1216 (2 × C—O_{stretch.}), 1084 (C—Cl_{stretch.}) cm^{−1}. ¹H NMR (300 MHz, DMSO-*d*₆): δ 11.72 (1H, bs, NH), 9.60 (1H, bs, OH), 8.02 (1H, s, H—C=N), 7.52–7.48 (4H, m, ArH), 7.33–7.28 (4H, m, ArH), 7.15 (1H, d, *J* = 1.8 Hz, ArH), 6.94 (1H, dd, *J* = 8.1, 1.8 Hz, ArH), 6.77 (1H, d, *J* = 8.1 Hz, ArH), 3.77 (3H, s, OCH₃). ¹³C NMR (75 MHz, DMSO-*d*₆): δ 172.6, 171.9, 166.4 (3 × C-triazine), 146.9 (H—C=N), 151.0, 149.4, 148.5, 130.3, 130.2, 130.0, 129.6, 126.0, 124.4, 124.3, 122.7, 115.8, 108.5 (13 × ArC), 55.7 (OCH₃). HRMS (ESI): *m/z* calcd for C₂₃H₁₇Cl₂N₅O₄ + H⁺: 498.0736 [M + H]⁺; found: 498.0729.

5.2.2.55 | 2-(2-(3-Chlorobenzylidene)-4,6-Bis(4-Chlorophenoxy)-1,3,5-Triazine (6j).

Yield: 76%; mp: 248°C–250°C; *R*_f: 0.77. IR (ATR, $\bar{\nu}$): 3241 (NH), 3060 (C_{sp2}—H_{stretch.}), 1615 (C=N), 1575, 1488 (2 × C=C), 1370, 1214 (2 × C—O_{stretch.}), 1086 (C—Cl_{stretch.}) cm^{−1}. ¹H NMR (300 MHz, DMSO-*d*₆): δ 12.01 (1H, s, NH), 8.13 (1H, s, H—C=N), 7.67 (1H, s, ArH), 7.56–7.44 (7H, m, ArH), 7.34–7.28 (4H, m, ArH). ¹³C NMR (75 MHz, DMSO-*d*₆): δ 172.6, 172.0, 167.0 (3 × C-triazine), 144.5 (H—C=N), 151.0, 136.9, 134.1, 131.2, 130.4, 130.3, 130.0, 129.7, 126.4, 126.2, 124.3 (11 × ArC). HRMS (ESI): *m/z* calcd for C₂₂H₁₄Cl₃N₅O₂ + Na⁺: 508.0111 [M + Na]⁺; found: 508.0107.

5.2.2.56 | 2-(2-(4-Chlorobenzylidene)-4,6-Bis(4-Chlorophenoxy)-1,3,5-Triazine (6k).

Yield: 75%; mp: 258°C–260°C; *R*_f: 0.77. IR (ATR, $\bar{\nu}$): 3233 (NH), 3061 (C_{sp2}—H_{stretch.}), 1615 (C=N), 1573, 1488 (2 × C=C), 1368, 1216 (2 × C—O_{stretch.}), 1086 (C—Cl_{stretch.}) cm^{−1}. ¹H NMR (300 MHz, DMSO-*d*₆): δ 11.96 (1H, s, NH), 8.15 (1H, s, H—C=N), 7.65 (2H, d, *J* = 8.4 Hz, ArH), 7.52–7.47 (6H, m, ArH), 7.33–7.27 (4H, m, ArH). ¹³C NMR (75 MHz, DMSO-*d*₆): δ 172.6, 171.9, 166.9 (3 × C-triazine), 145.1 (H—C=N), 151.0, 134.8, 133.6, 130.4, 129.9, 129.7, 129.4, 129.0, 124.2 (9 × ArC). HRMS (ESI): *m/z* calcd for C₂₂H₁₄Cl₃N₅O₂ + Na⁺: 508.0111 [M + Na]⁺; found: 508.0101.

5.2.2.57 | 4,6-Bis(4-Chlorophenoxy)-2-(2-(3-Nitrobenzylidene)Hydrazinyl)-1,3,5-Triazine (6l).

Yield: 70%; mp: 246°C–248°C; *R*_f: 0.75. IR (ATR, $\bar{\nu}$): 3233 (NH), 3050 (C_{sp2}—H_{stretch.}), 1615 (C=N), 1576, 1489 (2 × C=C), 1375, 1214 (2 × C—O_{stretch.}), 1092 (C—Cl_{stretch.}) cm^{−1}. ¹H NMR (300 MHz, DMSO-*d*₆): δ 12.13 (1H, s, NH), 8.46 (1H, s, ArH), 8.29–8.22 (2H, m, H—C=N, ArH), 8.03 (1H, d, *J* = 7.8 Hz, ArH), 7.70 (1H, t, *J* = 7.8 Hz, ArH), 7.53–7.48 (4H, m, ArH), 7.36–7.29 (4H, m, ArH). ¹³C NMR (75 MHz, DMSO-*d*₆): δ 172.6, 172.0, 167.0 (3 × C-triazine), 144.0 (H—C=N), 150.9, 148.6, 136.6, 133.8, 131.0, 130.4, 130.0, 129.7, 124.6, 124.2, 121.0 (11 × ArC). HRMS (ESI): *m/z* calcd for C₂₂H₁₄Cl₂N₆O₄ + Na⁺: 519.0351 [M + Na]⁺; found: 519.0340.

5.2.2.58 | 4,6-Bis(4-Chlorophenoxy)-2-(2-(4-Nitrobenzylidene)Hydrazinyl)-1,3,5-Triazine (6m).

Yield: 72%; mp: 231°C–233°C; *R*_f: 0.75. IR (ATR, $\bar{\nu}$): 3231 (NH), 3063 (C_{sp2}—H_{stretch.}), 1596 (C=N), 1572, 1484 (2 × C=C), 1369, 1197 (2 × C—O_{stretch.}), 1083 (C—Cl_{stretch.}) cm^{−1}. ¹H NMR (300 MHz, DMSO-*d*₆): δ 12.17 (1H, s, NH), 8.26 (3H, m, H—C=N, ArH), 7.88 (2H, d, *J* = 8.7 Hz, ArH), 7.54–7.48 (4H, m, ArH), 7.34–7.28 (4H, m, ArH). ¹³C NMR (75 MHz, DMSO-*d*₆): δ 172.7, 172.0, 167.1 (3 × C-triazine), 143.9 (H—C=N), 150.9, 148.1, 141.0, 130.3, 130.0,

129.8, 128.2, 124.5, 124.2 (9 × ArC). HRMS (ESI): m/z calcd for $C_{22}H_{14}Cl_2N_6O_4 + Na^+$: 519.0351 $[M + Na]^+$; found: 519.0346.

5.2.2.59 | 4,6-Bis(4-Chlorophenoxy)-2-(2-(Pyridin-3-Ylmethylene)Hydrazinyl)-1,3,5-Triazine (6n). Yield: 95%; mp: 232°C–234°C; R_f : 0.59. IR (ATR, $\bar{\nu}$): 3237 (NH), 3031 ($C_{sp2}-H_{stretch.}$), 1617 (C=N), 1564, 1487 ($2 \times C=C$), 1361, 1218 ($2 \times C-O_{stretch.}$), 1085 ($C-Cl_{stretch.}$) cm^{-1} . 1H NMR (300 MHz, DMSO- d_6): δ 12.04 (1H, s, NH), 8.76 (1H, d, $J = 1.8$ Hz, ArH), 8.58 (1H, dd, $J = 4.8, 1.5$ Hz, ArH), 8.20 (1H, s, H—C=N), 8.02 (1H, td, $J = 8.1, 1.8$ Hz, ArH), 7.50–7.43 (5H, m, ArH), 7.34–7.28 (4H, m, ArH). ^{13}C NMR (75 MHz, DMSO- d_6): δ 172.6, 171.9, 167.0 ($3 \times C$ -triazine), 143.7 (H—C=N), 151.1, 151.0, 148.9, 133.8, 130.6, 130.4, 130.3, 130.0, 129.7, 124.4, 124.2 (11 × ArC). HRMS (ESI): m/z calcd for $C_{21}H_{14}Cl_2N_6O_2 + H^+$: 453.0634 $[M + H]^+$; found: 453.0618

5.2.2.60 | 4,6-Bis(4-Chlorophenoxy)-2-(2-(Pyridin-4-Ylmethylene)Hydrazinyl)-1,3,5-Triazine (6o). Yield: 90%; mp: 304°C–306°C; R_f : 0.59. IR (ATR, $\bar{\nu}$): 3234 (NH), 3068 ($C_{sp2}-H_{stretch.}$), 1601 (C=N), 1559, 1486 ($2 \times C=C$), 1375, 1214 ($2 \times C-O_{stretch.}$), 1085 ($C-Cl_{stretch.}$) cm^{-1} . 1H NMR (300 MHz, DMSO- d_6): δ 12.13 (1H, s, NH), 8.62–8.60 (2H, d, $J = 5.7$ Hz, ArH), 8.13 (1H, s, H—C=N), 7.56–7.55 (2H, d, $J = 5.7$ Hz, ArH), 7.52–7.47 (4H, m, ArH), 7.33–7.27 (4H, m, ArH). ^{13}C NMR (75 MHz, DMSO- d_6): δ 172.7, 172.0, 167.1 ($3 \times C$ -triazine), 141.8 (H—C=N), 150.9, 150.7, 143.9, 130.4, 130.3, 130.0, 129.7, 124.2, 121.2 (9 × ArC). HRMS (ESI): m/z calcd for $C_{21}H_{14}Cl_2N_6O_2 + H^+$: 453.0634 $[M + H]^+$; found: 453.0624.

5.2.2.61 | 2-(2-Benzylidenehydrazinyl)-4,6-Bis(4-Bromophenoxy)-1,3,5-Triazine (7a). Yield: 86%; mp: 228°C–230°C; R_f : 0.69. IR (ATR, $\bar{\nu}$): 3231 (NH), 3103 ($C_{sp2}-H_{stretch.}$), 1603 (C=N), 1571, 1479 ($2 \times C=C$), 1368, 1189 ($2 \times C-O_{stretch.}$) cm^{-1} . 1H NMR (300 MHz, DMSO- d_6): δ 11.88 (1H, s, NH), 8.16 (1H, s, H—C=N), 7.65–7.60 (6H, m, ArH), 7.44–7.41 (3H, m, ArH), 7.28–7.21 (4H, m, ArH). ^{13}C NMR (75 MHz, DMSO- d_6): δ 172.5, 171.8, 166.8 ($3 \times C$ -triazine), 146.4 (H—C=N), 151.4, 134.6, 132.9, 132.6, 130.4, 129.2, 127.3, 124.6, 118.5, 118.3 (10 × ArC). HRMS (ESI): m/z calcd for $C_{22}H_{15}Br_2N_5O_2 + H^+$: 539.9671 $[M + H]^+$; found: 539.9659.

5.2.2.62 | 2-(2-(2-Hydroxybenzylidene)Hydrazinyl)-4,6-Bis(4-Bromophenoxy)-1,3,5-Triazine (7b). Yield: 80%; mp: 242°C–245°C; R_f : 0.62. IR (ATR, $\bar{\nu}$): 3350–2500 (br., OH), 3225 (NH), 3039 ($C_{sp2}-H_{stretch.}$), 1619 (C=N), 1588, 1480 ($2 \times C=C$), 1369, 1199 ($2 \times C-O_{stretch.}$) cm^{-1} . 1H NMR (300 MHz, DMSO- d_6): δ 12.14 (1H, s, NH), 10.89 (1H, s, OH), 8.32 (1H, s, H—C=N), 7.62 (4H, d, $J = 8.4$ Hz, ArH), 7.41 (1H, d, $J = 8.4$ Hz, ArH), 7.29–7.23 (5H, m, ArH), 6.90–6.85 (2H, m, ArH). ^{13}C NMR (75 MHz, DMSO- d_6): δ 172.5, 171.9, 166.3 ($3 \times C$ -triazine), 147.2 (H—C=N), 157.7, 151.4, 151.3, 132.9, 132.7, 131.7, 130.0, 129.3, 124.6, 124.5, 119.7, 118.8, 118.5, 116.9 (14 × ArC). HRMS (ESI): m/z calcd for $C_{22}H_{15}Br_2N_5O_3 + H^+$: 555.9620 $[M + H]^+$; found: 555.9611.

5.2.2.63 | 2-(2-(3-Hydroxybenzylidene)Hydrazinyl)-4,6-Bis(4-Bromophenoxy)-1,3,5-Triazine (7c). Yield: 71%; mp: 252°C–254°C; R_f : 0.60. IR (ATR, $\bar{\nu}$): 3500–2500 (br., OH), 3223 (NH), 3074 ($C_{sp2}-H_{stretch.}$), 1607 (C=N), 1565, 1480 ($2 \times C=C$), 1367, 1195 ($2 \times C-O_{stretch.}$) cm^{-1} . 1H NMR (300 MHz, DMSO- d_6): δ 11.81 (1H, s, NH), 9.61 (1H, s, OH), 8.08 (1H, s, H—C=N), 7.62 (4H, m, ArH), 7.27–7.19 (5H, m, ArH), 7.13 (1H, s, ArH), 7.00

(1H, d, $J = 7.2$ Hz, ArH), 6.80 (1H, dd, $J = 8.1, 2.4$ Hz, ArH). ^{13}C NMR (75 MHz, DMSO- d_6): δ 172.5, 171.7, 166.8 ($3 \times C$ -triazine), 146.2 (H—C=N), 158.1, 151.4, 135.8, 132.8, 132.6, 130.3, 124.6, 119.0, 118.5, 118.3, 117.8, 113.0 (12 × ArC). HRMS (ESI): m/z calcd for $C_{22}H_{15}Br_2N_5O_3 + H^+$: 555.9620 $[M + H]^+$; found: 555.9607.

5.2.2.64 | 2-(2-(4-Hydroxybenzylidene)Hydrazinyl)-4,6-Bis(4-Bromophenoxy)-1,3,5-Triazine (7d). Yield: 69%; mp: 196°C–198°C; R_f : 0.66. IR (ATR, $\bar{\nu}$): 3500–2500 (br., OH), 3243 (NH), 3058 ($C_{sp2}-H_{stretch.}$), 1602 (C=N), 1568, 1484 ($2 \times C=C$), 1370, 1214 ($2 \times C-O_{stretch.}$) cm^{-1} . 1H NMR (300 MHz, DMSO- d_6): δ 11.68 (1H, s, NH), 9.94 (1H, s, OH), 8.06 (1H, s, H—C=N), 7.64–7.59 (4H, m, ArH), 7.45 (2H, d, $J = 8.7$ Hz, ArH), 7.26–7.20 (4H, m, ArH), 6.80 (2H, d, $J = 8.7$ Hz, ArH). ^{13}C NMR (75 MHz, DMSO- d_6): δ 172.5, 171.6, 166.5 ($3 \times C$ -triazine), 146.9 (H—C=N), 159.8, 151.5, 132.8, 132.6, 129.1, 125.6, 124.7, 124.6, 118.4, 118.3, 116.1 (11 × ArC). HRMS (ESI): m/z calcd for $C_{22}H_{15}Br_2N_5O_3 + H^+$: 555.9620 $[M + H]^+$; found: 555.9606.

5.2.2.65 | 4,6-Bis(4-Bromophenoxy)-2-(2-(4-Methoxybenzylidene)Hydrazinyl)-1,3,5-Triazine (7e). Yield: 67%; mp: 259°C–261°C; R_f : 0.70. IR (ATR, $\bar{\nu}$): 3250 (NH), 3057 ($C_{sp2}-H_{stretch.}$), 2998 ($C_{sp3}-H_{stretch.}$), 1608 (C=N), 1568, 1485 ($2 \times C=C$), 1371, 1217 ($2 \times C-O_{stretch.}$) cm^{-1} . 1H NMR (300 MHz, DMSO- d_6): δ 11.74 (1H, s, NH), 8.10 (1H, s, H—C=N), 7.64–7.55 (6H, m, ArH), 7.26–7.20 (4H, m, ArH), 6.97 (2H, d, $J = 8.7$ Hz, ArH), 3.79 (3H, s, OCH₃). ^{13}C NMR (75 MHz, DMSO- d_6): δ 172.5, 171.7, 166.6 ($3 \times C$ -triazine), 146.5 (H—C=N), 161.2, 151.5, 132.8, 132.6, 129.0, 127.2, 124.6, 118.4, 118.3, 114.7 (10 × ArC), 55.7 (OCH₃). HRMS (ESI): m/z calcd for $C_{23}H_{17}Br_2N_5O_3 + H^+$: 569.9776 $[M + H]^+$; found: 569.9761.

5.2.2.66 | 4,6-Bis(4-Bromophenoxy)-2-(2-(4-Methylbenzylidene)Hydrazinyl)-1,3,5-Triazine (7f). Yield: 80%; mp: 260°C–262°C; R_f : 0.75. IR (ATR, $\bar{\nu}$): 3237 (NH), 3058 ($C_{sp2}-H_{stretch.}$), 2913 ($C_{sp3}-H_{stretch.}$), 1588 (C=N), 1568, 1484 ($2 \times C=C$), 1368, 1212 ($2 \times C-O_{stretch.}$) cm^{-1} . 1H NMR (300 MHz, CDCl₃): δ 7.89 (1H, s, H—C=N), 7.60 (2H, d, $J = 8.1$ Hz, ArH), 7.53–7.50 (4H, m, ArH), 7.21 (2H, d, $J = 7.8$ Hz, ArH), 7.13–7.02 (4H, m, ArH), 2.32 (3H, s, CH₃). ^{13}C NMR (75 MHz, DMSO- d_6): δ 172.5, 171.7, 166.7 ($3 \times C$ -triazine), 146.6 (H—C=N), 151.4, 140.2, 132.8, 132.6, 131.9, 129.8, 127.3, 124.6, 118.5, 118.3 (10 × ArC), 21.4 (CH₃). HRMS (ESI): m/z calcd for $C_{23}H_{17}Br_2N_5O_2 + H^+$: 553.9827 $[M + H]^+$; found: 553.9820.

5.2.2.67 | 2-(2-(4-*N,N*-Dimethylaminobenzylidene)Hydrazinyl)-4,6-Bis(4-Bromophenoxy)-1,3,5-Triazine (7g). Yield: 93%; mp: 226°C–228°C; R_f : 0.68. IR (ATR, $\bar{\nu}$): 3248 (NH), 3040 ($C_{sp2}-H_{stretch.}$), 2895 ($C_{sp3}-H_{stretch.}$), 1596 (C=N), 1567, 1479 ($2 \times C=C$), 1364, 1200 ($2 \times C-O_{stretch.}$) cm^{-1} . 1H NMR (300 MHz, DMSO- d_6): δ 11.56 (1H, s, NH), 8.03 (1H, s, H—C=N), 7.64–7.59 (4H, m, ArH), 7.43 (2H, d, $J = 9.0$ Hz, ArH), 7.26–7.20 (4H, m, ArH), 6.71 (2H, d, $J = 9.0$ Hz, ArH), 2.96 (6H, s, N(CH₃)₂). ^{13}C NMR (75 MHz, DMSO- d_6): δ 172.5, 171.5, 166.2 ($3 \times C$ -triazine), 147.5 (H—C=N), 151.8, 151.5, 132.8, 132.6, 128.7, 124.6, 121.9, 118.4, 118.2, 112.1 (10 × ArC), 40.3 (N(CH₃)₂). HRMS (ESI): m/z calcd for $C_{24}H_{20}Br_2N_6O_2 + H^+$: 583.0093 $[M + H]^+$; found: 583.0078.

5.2.2.68 | 4,6-Bis(4-Bromophenoxy)-2-(2-((*E*)-3-Phenylallylidene)Hydrazinyl)-1,3,5-Triazine (7h). Yield: 91%; mp: 256°C–258°C; R_f : 0.65. IR (ATR, $\bar{\nu}$): 3217 (NH), 3060

($C_{sp^2}-H_{stretch.}$), 1610 (C=N), 1571, 1484 ($2 \times C=C$), 1367, 1205 ($2 \times C-O_{stretch.}$) cm^{-1} . 1H NMR (300 MHz, DMSO- d_6): δ 11.74 (1H, s, NH), 7.99 (1H, dd, $J = 4.8, 3.6$ Hz, H-C=N), 7.64–7.59 (6H, m, ArH), 7.40–7.31 (3H, m, ArH), 7.25–7.20 (4H, m, ArH), 6.99–6.97 (2H, m, (CH=CHAr)). ^{13}C NMR (75 MHz, DMSO- d_6): δ 172.5, 171.7, 166.6 ($3 \times C$ -triazine), 149.2 (H-C=N), 136.3 (CH=CHAr), 125.7 (CH=CHAr), 151.4, 139.5, 132.9, 132.7, 129.2, 127.5, 124.5, 118.5, 118.3 (9 \times ArC). HRMS (ESI): m/z calcd for $C_{24}H_{17}Br_2N_5O_2 + Na^+$: 587.9647 [M + Na] $^+$; found: 587.9631.

5.2.2.69 | 2-(2-(4-Hydroxy-3-Methoxybenzylidene)Hydrazinyl)-4,6-Bis(4-Bromophenoxy)-1,3,5-Triazine (7i). Yield: 77%; mp: 223°C–224°C; R_f : 0.69. IR (ATR, $\bar{\nu}$): 3416 (br., OH), 3229 (NH), 3058 ($C_{sp^2}-H_{stretch.}$), 2929 ($C_{sp^3}-H_{stretch.}$), 1605 (C=N), 1572, 1486 ($2 \times C=C$), 1368, 1215 ($2 \times C-O_{stretch.}$) cm^{-1} . 1H NMR (300 MHz, DMSO- d_6): δ 11.70 (1H, bs, NH), 9.55 (1H, bs, OH), 8.02 (1H, s, H-C=N), 7.64–7.61 (4H, m, ArH), 7.28–7.22 (4H, m, ArH), 7.16 (1H, d, $J = 1.5$ Hz, ArH), 6.95 (1H, dd, $J = 8.1, 1.5$ Hz, ArH), 6.79 (1H, d, $J = 8.1$ Hz, ArH), 3.78 (3H, s, OCH $_3$). ^{13}C NMR (75 MHz, DMSO- d_6): δ 172.4, 171.8, 166.4 ($3 \times C$ -triazine), 151.5, 151.4, 146.9 (H-C=N), 149.3, 148.4, 132.9, 132.5, 126.0, 124.8, 124.7, 122.6, 118.5, 118.2, 115.7, 108.5 (12 \times ArC), 55.8 (OCH $_3$). HRMS (ESI): m/z calcd for $C_{23}H_{17}Br_2N_5O_4 + H^+$: 585.9726 [M + H] $^+$; found: 585.9711.

5.2.2.70 | 4,6-Bis(4-Bromophenoxy)-2-(2-(3-Chlorobenzylidene)Hydrazinyl)-1,3,5-Triazine (7j). Yield: 69%; mp: 267°C–269°C; R_f : 0.72. IR (ATR, $\bar{\nu}$): 3237 (NH), 3056 ($C_{sp^2}-H_{stretch.}$), 1613 (C=N), 1572, 1485 ($2 \times C=C$), 1369, 1209 ($2 \times C-O_{stretch.}$) cm^{-1} . 1H NMR (300 MHz, DMSO- d_6): δ 12.01 (1H, s, NH), 8.12 (1H, s, H-C=N), 7.68–7.61 (5H, m, ArH), 7.57–7.53 (1H, m, ArH), 7.46–7.44 (2H, m, ArH), 7.29–7.22 (4H, m, ArH). ^{13}C NMR (75 MHz, DMSO- d_6): δ 172.5, 171.9, 166.9 ($3 \times C$ -triazine), 144.5 (H-C=N), 151.4, 136.9, 134.1, 132.9, 132.6, 131.1, 130.0, 126.4, 126.2, 124.6, 118.5, 118.4 (12 \times ArC). HRMS (ESI): m/z calcd for $C_{22}H_{14}Br_2ClN_5O_2 + Na^+$: 595.9100 [M + Na] $^+$; found: 595.9089.

5.2.2.71 | 4,6-Bis(4-Bromophenoxy)-2-(2-(4-Chlorobenzylidene)Hydrazinyl)-1,3,5-Triazine (7k). Yield: 70%; mp: 256°C–258°C; R_f : 0.73. IR (ATR, $\bar{\nu}$): 3226 (NH), 3090 ($C_{sp^2}-H_{stretch.}$), 1614 (C=N), 1571, 1485 ($2 \times C=C$), 1372, 1210 ($2 \times C-O_{stretch.}$) cm^{-1} . 1H NMR (300 MHz, DMSO- d_6): δ 11.94 (1H, s, NH), 8.15 (1H, s, H-C=N), 7.66–7.60 (6H, m, ArH), 7.48 (2H, d, $J = 8.4$ Hz, ArH), 7.27–7.21 (4H, m, ArH). ^{13}C NMR (75 MHz, DMSO- d_6): δ 172.5, 171.8, 166.9 ($3 \times C$ -triazine), 145.1 (H-C=N), 151.4, 134.8, 133.6, 132.9, 132.6, 129.3, 128.9, 124.6, 118.5, 118.4 (10 \times ArC). HRMS (ESI): m/z calcd for $C_{22}H_{14}Br_2ClN_5O_2 + Na^+$: 595.9100 [M + Na] $^+$; found: 595.9080.

5.2.2.72 | 4,6-Bis(4-Bromophenoxy)-2-(2-(3-Nitrobenzylidene)Hydrazinyl)-1,3,5-Triazine (7l). Yield: 65%; mp: 246°C–248°C; R_f : 0.60. IR (ATR, $\bar{\nu}$): 3308 (NH), 3091 ($C_{sp^2}-H_{stretch.}$), 1586 (C=N), 1562, 1485 ($2 \times C=C$), 1369, 1197 ($2 \times C-O_{stretch.}$) cm^{-1} . 1H NMR (300 MHz, DMSO- d_6): δ 12.11 (1H, s, NH), 8.45 (1H, t, $J = 7.8$ Hz, ArH), 8.26–8.21 (2H, m, H-C=N, ArH), 8.02 (1H, d, $J = 7.8$ Hz, ArH), 7.73–7.60 (5H, m, ArH), 7.30–7.22 (4H, m, ArH). ^{13}C NMR (75 MHz, DMSO- d_6): δ 172.5, 171.9, 167.0 ($3 \times C$ -triazine), 144.0 (H-C=N), 151.4, 148.6, 136.4, 133.7, 132.9, 132.6, 130.8, 124.6, 121.0, 118.5, 118.4 (11 \times ArC). HRMS (ESI): m/z calcd for $C_{22}H_{14}Br_2N_6O_4 + Na^+$: 606.9341 [M + Na] $^+$; found: 606.9328.

5.2.2.73 | 4,6-Bis(4-Bromophenoxy)-2-(2-(4-Nitrobenzylidene)Hydrazinyl)-1,3,5-Triazine (7m). Yield: 67%; mp: 240°C–242°C; R_f : 0.61. IR (ATR, $\bar{\nu}$): 3233 (NH), 3053 ($C_{sp^2}-H_{stretch.}$), 1604 (C=N), 1570, 1485 ($2 \times C=C$), 1367, 1193 ($2 \times C-O_{stretch.}$) cm^{-1} . 1H NMR (300 MHz, DMSO- d_6): δ 12.13 (1H, s, NH), 8.30–8.20 (3H, m, H-C=N, ArH), 7.82 (2H, d, $J = 8.4$ Hz, ArH), 7.64–7.59 (4H, m, ArH), 7.28–7.22 (4H, m, ArH). ^{13}C NMR (75 MHz, DMSO- d_6): δ 172.5, 171.9, 167.0 ($3 \times C$ -triazine), 143.7 (H-C=N), 151.4, 147.9, 140.9, 132.8, 132.6, 128.1, 124.6, 124.3, 118.5, 118.4 (12 \times ArC). HRMS (ESI): m/z calcd for $C_{22}H_{14}Br_2N_6O_4 + Na^+$: 606.9341 [M + Na] $^+$; found: 606.9332.

5.2.2.74 | 4,6-Bis(4-Bromophenoxy)-2-(2-(Pyridin-3-Ylmethylene)Hydrazinyl)-1,3,5-Triazine (7n). Yield: 96%; mp: 335°C–337°C; R_f : 0.57. IR (ATR, $\bar{\nu}$): 3061 ($C_{sp^2}-H_{stretch.}$), 1595 (C=N), 1561, 1482 ($2 \times C=C$), 1381, 1208 ($2 \times C-O_{stretch.}$) cm^{-1} . 1H NMR (300 MHz, DMSO- d_6): δ 12.05 (1H, s, NH), 8.76 (1H, d, $J = 1.8$ Hz, ArH), 8.58 (1H, dd, $J = 4.8, 1.8$ Hz, ArH), 8.19 (1H, s, H-C=N), 8.02 (1H, td, $J = 8.1, 1.8$ Hz, ArH), 7.65–7.61 (4H, m, ArH), 7.45 (1H, dd, $J = 8.1, 4.8$ Hz, ArH), 7.28–7.21 (4H, m, ArH). ^{13}C NMR (75 MHz, DMSO- d_6): δ 172.5, 171.8, 166.9 ($3 \times C$ -triazine), 143.7 (H-C=N), 151.4, 151.0, 148.9, 133.7, 132.9, 132.6, 130.5, 124.6, 124.4, 118.5, 118.4 (11 \times ArC). HRMS (ESI): m/z calcd for $C_{21}H_{14}Br_2N_6O_2 + H^+$: 540.9623 [M + H] $^+$; found: 540.9611.

5.2.2.75 | 4,6-Bis(4-Bromophenoxy)-2-(2-(Pyridin-4-Ylmethylene)Hydrazinyl)-1,3,5-Triazine (7o). Yield: 90%; mp: 274°C–276°C; R_f : 0.56. IR (ATR, $\bar{\nu}$): 3062 ($C_{sp^2}-H_{stretch.}$), 1557 (C=N), 1483, 1445 ($2 \times C=C$), 1376, 1205 ($2 \times C-O_{stretch.}$) cm^{-1} . 1H NMR (300 MHz, DMSO- d_6): δ 12.14 (1H, s, NH), 8.61 (2H, d, $J = 4.8$ Hz, ArH), 8.13 (1H, s, H-C=N), 7.65–7.61 (4H, m, ArH), 7.55 (2H, d, $J = 4.8$, ArH), 7.27–7.22 (4H, m, ArH). ^{13}C NMR (75 MHz, DMSO- d_6): δ 172.6, 171.9, 167.1 ($3 \times C$ -triazine), 143.8 (H-C=N), 151.4, 150.6, 141.8, 132.9, 132.7, 124.6, 121.2, 118.5, 118.4 (9 \times ArC). HRMS (ESI): m/z calcd for $C_{21}H_{14}Br_2N_6O_2 + H^+$: 540.9623 [M + H] $^+$; found: 540.9612.

5.3 | Biological Evaluation

5.3.1 | DNA Interactions Studies

5.3.1.1 | Purification and Preparation of DNA Solution. A Salmon Sperm DNA solution (2.5 mg) was dissolved in 10 mL deionized water and stirred for 24 h in order to prepare 234 mM solution of DNA. Concentration of DNA solution was measured employing UV-visible spectroscopy using Beer's Lambert law. The absorbance of the DNA solution was recorded at two different wavelengths, that is, 260 and 280 nm. The ratio of two absorbances A_{260}/A_{280} indicates the purity of DNA solution. The absorbance ratio was between 1.7 and 1.9 indicating that DNA solution was free from contamination.

5.3.1.2 | Preparation of Stock Solution for Test Compounds. The stock solution (200 mM) of the test compound was prepared by dissolving calculated amount of each compound in DMSO.

5.3.1.3 | Evaluation of Thermodynamic and Kinetic Parameters. The antineoplastic activities of a drug are based on its binding or denaturation of DNA and interfering abilities

of the drug in DNA processes. Hence, the absorbance of a test compound is quantified following its absorption on incremental increase of DNA concentrations, while keeping the compound concentration constant. The binding constant (K_b) may be calculated from the intercept to slope ratio of the plot of $A_o/(A - A_o)$ versus $1/[DNA]$ using Benesi-Hildebr and formula [55].

$$\frac{A_o}{A - A_o} = \frac{\epsilon_G}{\epsilon_{H-G} - \epsilon_G} + \frac{\epsilon_G}{\epsilon_{H-G} - \epsilon_G} \times \frac{1}{K_b [DNA]}$$

where A_o is the absorption of free compound and A is the absorption of compound-DNA adduct. ϵ_G and ϵ_{H-G} correspond to extinction coefficients (molar) of the complex and drug-DNA adduct, respectively.

5.3.1.4 | In Vitro Antiproliferative Evaluation.

5.3.1.4.1 | Cancer Cell Culture. The human cancer cell lines used in this study including Capan-1, HCT-116, LN-229, NCI-H460, HL-60, K-562, H, and Z-138 were sourced from the American Type Culture Collection (ATCC, Manassas, VA, USA). The DND-41 cell line was obtained from the Deutsche Sammlung von Mikroorganismen und Zellkulturen (DSMZ Leibniz Institute, Germany). Culture media were provided by Gibco Life Technologies, USA, and supplemented with 10% fetal bovine serum (HyClone, GE Healthcare Life Sciences, USA), while media for other cell lines were acquired from Sigma.

5.3.1.4.2 | Proliferation Assays. Adherent cell lines—including LN-229, HCT-116, NCI-H460, and Capan-1—were seeded into 384-well tissue culture plates (Greiner) at densities ranging from 500 to 1500 cells per well. After overnight incubation, cells were treated with a series of seven concentrations of test compounds, spanning from 100 to 0.006 μ M. Suspension cell lines, including HL-60, K-562, Z-138, and DND-41, were plated in 384-well plates at densities of 2500–5500 cells per well and exposed to the same concentration range. Following 72 h of compound exposure, cell viability was assessed using the CellTiter 96 AQueous one solution cell proliferation assay (MTS) reagent (Promega), in accordance with the manufacturer's instructions. Absorbance was measured at 490 nm using a SpectraMax Plus 384 plate reader (Molecular Devices), and the resulting optical density (OD) values were used to calculate the IC_{50} . All compounds were tested in two independent experiments.

For HeLa cells, assays were conducted in 96-well microtiter plates with seeding densities between 1×10^4 and 3×10^4 cells/mL, adjusted according to the cell line's doubling time. Test compounds were freshly prepared on the day of treatment and applied in five 10-fold serial dilutions (10^{-8} – 10^{-4} M). After 72 h of incubation, cell viability was evaluated using the MTS assay as described. Absorbance was read at 570 nm, and OD values were used to determine IC_{50} values. Each assay was performed in duplicate and repeated in at least two independent experiments.

5.3.1.4.3 | Molecular Docking Simulations. Molecular docking simulations were performed using the AutoDock program. Protein structures were preprocessed with UCSF

Chimera 1.15 [56], and docking was carried out using the Lamarckian genetic algorithm (LGA) with 2 500 000 energy evaluations per run. Docking scores were calculated using AutoDock's default scoring function, and grid maps were generated using AutoGrid. The docking results were visualized and analyzed with BIOVIA Discovery Studio 2020 [57]. To validate the docking protocol, each simulation was conducted using the native ligands co-crystallized in the respective protein structures. The method successfully reproduced the native ligand–protein binding geometries. Figure 3 shows the comparison between the native ligands of 5X74, 4VB, and 5E8O and their corresponding redocked poses generated by AutoDock.

6 | Conclusions

A novel series of 2-(2-(arylbenzylidenehydrazinyl)-4,6-(substituted-diphenoxy)-1,3,5-triazine derivatives (**3a–o** to **7a–o**) was successfully synthesized. Selected analogues from this series were evaluated for their anticancer activity against eight human cancer cell lines: Capan-1, HCT-116, LN229, NCI-H460, DND-41, HL-60, K562, and Z138. Among the tested compounds, **5i** and **7b** exhibited potent cytotoxic effects, demonstrating low micromolar IC_{50} values of 2.4 and 1.9 μ M, respectively, against pancreatic adenocarcinoma (Capan-1). Notably, compound **5i** also showed significant activity against colorectal carcinoma (HCT-116), with an IC_{50} of 2.2 μ M. All synthesized compounds (**3a–o** to **7a–o**) were further investigated for their DNA-binding affinity using UV–visible spectroscopy, and the binding constants were determined graphically. Most compounds exhibited strong interactions with DNA, as indicated by high Gibbs free energy values, reflecting spontaneous binding and the formation of stable complexes. Computational studies revealed that compound **7b** possessed the highest total binding energy and the lowest inhibition constant (K_i) among the tested compounds, which correlated well with its in vitro anticancer activity. Molecular docking results supported these findings, and MD simulations confirmed the structural stability of the **7b**–PDE δ complex (PDB ID: 5E80), with a critical interaction distance of 0.9 Å maintaining protein integrity throughout the simulation. These results highlight compounds **5i** and **7b** as promising lead candidates for further development as anticancer agents, particularly targeting pancreatic (Capan-1) and colorectal (HCT-116) carcinomas, due to their potent cytotoxicity and strong DNA-binding capabilities.

Acknowledgments

We acknowledge Leentje Persoons and Dirk Daelemans from the Laboratory of Virology and Chemotherapy, KU Leuven, Belgium for the antitumoral testing of the compounds.

Conflicts of Interest

The authors declare no conflicts of interest.

Data Availability Statement

The authors have nothing to report.

References

1. J. Kumawat, S. Jain, N. Misra, J. Dwivedi, and D. Kishore, "1,3,5-Triazine: Recent Development in Synthesis of Its Analogs and Biological Profile," *Mini-Reviews in Medicinal Chemistry* 24 (2024): 2019–2071.
2. N. B. Ayrim, F. R. Hafedh, Y. M. Kadhim, et al., "Hexahydro-1,2,3-Triazine Derivatives: Synthesis, Antimicrobial Evaluation, Antibiofilm Activity and Study of Molecular Docking Against Glucosamine-6-Phosphate," *Indonesian Journal of Chemistry* 24 (2024): 141–151.
3. H. Liu, S. Long, K. P. Rakesh, and G.-F. Zha, "Structure-Activity Relationships (SAR) of Triazine Derivatives: Promising Antimicrobial Agents," *European Journal of Medicinal Chemistry* 185 (2020): 111804.
4. S. Cascioferro, B. Parrino, V. Spanò, et al., "1,3,5-Triazines: A Promising Scaffold for Anticancer Drugs Development," *European Journal of Medicinal Chemistry* 142 (2017): 523–549.
5. A. El-Faham, M. Farooq, Z. Almarhoon, et al., "Di- and Tri-Substituted s-Triazine Derivatives: Synthesis, Characterization, Anticancer Activity in Human Breast-Cancer Cell Lines, and Developmental Toxicity in Zebrafish Embryos," *Bioorganic Chemistry* 94 (2020): 103397.
6. M. Farooq, A. Sharma, Z. Almarhoon, et al., "Design and Synthesis of Mono- and Di-Pyrazolyl-s-Triazine Derivatives, Their Anticancer Profile in Human Cancer Cell Lines, and In Vivo Toxicity in Zebrafish Embryos," *Bioorganic Chemistry* 87 (2019): 457–464.
7. D. Rageot, T. Bohnacker, E. Keles, et al., "(S)-4-(Difluoromethyl)-5-(4-(3-Methylmorpholino)-6-Morpholino-1,3,5-Triazin-2-Yl)Pyridin-2-Amine (PQR530), a Potent, Orally Bioavailable, and Brain-Penetrable Dual Inhibitor of Class I PI3K and mTOR Kinase," *Journal of Medicinal Chemistry* 62 (2019): 6241–6261.
8. D. R. Shah, R. P. Modh, and K. H. Chikhalia, "Privileged s-Triazines: Structure and Pharmacological Applications," *Future Medicinal Chemistry* 6 (2014): 463–477.
9. O. Sharma, S. Srivastava, M. Sharma, and R. Malik, "1,3,5-Triazine Derivatives as Potential Anticancer Agents Against Lung and Breast Cancer Cell Lines: Synthesis, Biological Evaluation, and Structure-Based Drug Design Studies," *Journal of Molecular Structure* 1308 (2024): 138078.
10. M. Shanmugam, K. Narayanan, K. H. Prasad, et al., "Synthesis, Characterization, and Antiproliferative and Apoptosis Inducing Effects of Novel s-Triazine Derivatives," *New Journal of Chemistry* 42 (2018): 1698–1714.
11. M. Balaha, M. El-Hamamsy, N. El-Din, and N. A. El-Mahdy, "Synthesis, Evaluation and Docking Study of 1,3,5-Triazine Derivatives as Cytotoxic Agents Against Lung Cancer," *Journal of Applied Pharmaceutical Science* 6 (2016): 28–45.
12. L. Bai, C. Wei, J. Zhang, and R. Song, "Design, Synthesis, and Anti-PVY Biological Activity of 1,3,5-Triazine Derivatives Containing Piperazine Structure," *International Journal of Molecular Sciences* 24 (2023): 8280.
13. B. Klenke, "Antiplasmodial Activity of a Series of 1,3,5-Triazine-Substituted Polyamines," *Journal of Antimicrobial Chemotherapy* 52 (2023): 290–293.
14. A. Agarwal, K. Srivastava, S. K. Puri, and P. M. Chauhan, "Syntheses of 2,4,6-Trisubstituted Triazines as Antimalarial Agents," *Bioorganic & Medicinal Chemistry* 15 (2005): 531–533.
15. D. Tripathi, A. R. Mishra, D. Singh, and A. K. Dwivedi, "Synthesis of New Fungitoxic 2-Aryl-1,3,4-Oxadiazolo [3,2-a]-s-Triazine-5,7-Dithiones and Their 6-Aryl Sulphonyl Derivatives," *Indian Journal of Heterocyclic Chemistry* 16 (2007): 239–242.
16. L. Marín-Ocampo, L. A. Veloza, R. Abonia, and J. C. Sepúlveda-Arias, "Anti-Inflammatory Activity of Triazine Derivatives: A Systematic Review," *European Journal of Medicinal Chemistry* 162 (2019): 435–447.
17. S. Singh, H. R. Bhat, M. K. Kumawat, and U. P. Singh, "Discovery of Novel 1,3,5-Triazine-Thiazolidine-2,4-Diones as Dipeptidyl Peptidase-4 Inhibitors With Antibacterial Activity Targeting the S1 Pocket for the Treatment of Type 2 Diabetes," *RSC Advances* 5 (2015): 14095–14102.
18. J. K. Srivastava, N. T. Awatade, H. R. Bhat, et al., "Pharmacological Evaluation of Hybrid Thiazolidin-4-One-1, 3, 5-Triazines for NF- κ B, Biofilm and CFTR Activity," *RSC Advances* 5 (2015): 88710–88718.
19. Z. Nie, C. Perretta, P. Erickson, et al., "Structure-Based Design and Synthesis of Novel Macrocyclic Pyrazolo[1,5-a] [1,3,5]Triazine Compounds as Potent Inhibitors of Protein Kinase CK2 and Their Anticancer Activities," *Bioorganic & Medicinal Chemistry Letters* 18 (2008): 619–623.
20. Q. Dai, Q. Sun, X. Ouyang, et al., "Antitumor Activity of s-Triazine Derivatives: A Systematic Review," *Molecules* 28 (2023): 4278.
21. J. R. Wong, L. M. Morton, M. A. Tucker, et al., "Risk of Subsequent Malignant Neoplasms in Long-Term Hereditary Retinoblastoma Survivors After Chemotherapy and Radiotherapy," *Journal of Clinical Oncology* 32 (2014): 3284–3290.
22. D. H. Moore, F. Valea, L. S. Crumpler, and W. C. Fowler, "Hexamethylmelamine/Altretamine as Second-Line Therapy for Epithelial Ovarian Carcinoma," *Gynecologic Oncology* 51 (1993): 109–112.
23. M. Koh, J. C. Lee, C. Min, and A. Moon, "A Novel Metformin Derivative, HL010183, Inhibits Proliferation and Invasion of Triple-Negative Breast Cancer Cells," *Bioorganic & Medicinal Chemistry* 21 (2013): 2305–2313.
24. S. D. Phadke, M. Yu, K. Miller, A. N. Shah, O. C. Danciu, and K. B. Wisinski, "Results of the Safety Run-In of Gedatolisib Plus Talazoparib in Advanced Triple Negative or BRCA 1/2 Positive HER2 Negative Breast Cancer," *Journal of Clinical Oncology* 40 (2022): e13075.
25. I. A. Malik, "Altretamine Is an Effective Palliative Therapy of Patients With Recurrent Epithelial Ovarian Cancer," *Japanese Journal of Clinical Oncology* 31 (2001): 69–73.
26. N. Keldsen, H. Havsteen, I. Vergote, K. Bertelsen, and A. Jakobsen, "Altretamine (Hexamethylmelamine) in the Treatment of Platinum-Resistant Ovarian Cancer: A Phase II Study," *Gynecologic Oncology* 88 (2003): 118–122.
27. A. Kajal, S. Bala, S. Kamboj, N. Sharma, and V. Saini, "Schiff Bases: A Versatile Pharmacophore," *Journal of Catalysis* 2013 (2013): 893512.
28. A. Barakat, F. F. El-Senduny, Z. Almarhoon, et al., "Synthesis, X-Ray Crystal Structures, and Preliminary Antiproliferative Activities of New s-Triazine-Hydroxybenzylidene Hydrazone Derivatives," *Journal of Chemistry* 2019 (2019): 9403908.
29. H. H. Al Rasheed, A. M. Malebari, K. A. Dahlous, and A. El-Faham, "Synthesis and Characterization of New Series of 1,3-5-Triazine Hydrazone Derivatives With Promising Antiproliferative Activity," *Molecules* 25 (2020): 2708.
30. H. H. Al Rasheed, A. M. Malebari, K. A. Dahlous, D. Fayne, and A. El-Faham, "Synthesis, Anti-Proliferative Activity, and Molecular Docking Study of New Series of 1,3-5-Triazine Schiff Base Derivatives," *Molecules* 25 (2020): 4065.
31. P. Rozbicki, E. Oğuz, E. Wolińska, F. Türkan, A. Cetin, and D. Branowska, "Synthesis and Examination of 1,2,4-Triazine-Sulfonamide Hybrids as Potential Inhibitory Drugs: Inhibition Effects on AChE and GST Enzymes In Silico and In Vitro Conditions," *Archiv der Pharmazie* 357 (2024): 2009182.
32. A. El-Faham, S. M. Soliman, H. A. Ghabbour, et al., "Ultrasonic Promoted Synthesis of Novel s-Triazine-Schiff Base Derivatives; Molecular Structure, Spectroscopic Studies and Their Preliminary Anti-Proliferative Activities," *Journal of Molecular Structure* 112 (2016): 121–135.
33. F. Türkan, A. Cetin, P. Rozbicki, E. Oğuz, E. Wolińska, and D. Branowska, "Pharmacological Assessment of Disulfide-Triazine Hybrids: Synthesis, Enzyme Inhibition, and Molecular Docking Study," *Medicinal Chemistry Research* 33 (2024): 1205–1217.
34. S. Asghar, S. Hameed, N. A. Al-Masoudi, B. Saeed, and A. Shtaiwi, "Design, Synthesis, Docking Studies and Molecular Dynamics Simulation of New 1,3,5-Triazine Derivatives as Anticancer Agents Selectively Targeting Pancreatic Adenocarcinoma (Capan-1)," *Chemistry & Biodiversity* 21 (2024): e202400112.

35. S. Asghar, S. Hameed, M. N. Tahir, and M. M. Naseer, "Molecular Duplexes Featuring NH... N, CH... O and CH... π Interactions in Solid-state Self-assembly of Triazine-based Compounds," *Royal Society Open Science* 9 (2022): 220603.
36. K. Cheung-Ong, G. Giaever, and C. Nislow, "DNA-damaging Agents in Cancer Chemotherapy: Serendipity and Chemical Biology," *Chemistry & Biology* 20 (2013): 648–659.
37. M. T. Schweizer and E. S. Antonarakis, "Prognostic and Therapeutic Implications of DNA Repair Gene Mutations in Advanced Prostate Cancer," *Clinical Advances in Hematology & Oncology* 15 (2017): 785–795.
38. D. Kim, Y. Liu, S. Oberly, R. Freire, and M. B. Smolka, "ATR-Mediated Proteome Remodeling Is a Major Determinant of Homologous Recombination Capacity in Cancer Cells," *Nucleic Acids Research* 46 (2018): 8311–8325.
39. K. Watanabe and N. Seki, "Biology and Development of DNA-Targeted Drugs, Focusing on Synthetic Lethality, DNA Repair, and Epigenetic Modifications for Cancer: A Review," *International Journal of Molecular Sciences* 25 (2024): 752.
40. M. Sirajuddin, S. Ali, and A. Badshah, "Drug–DNA Interactions and Their Study by UV–Visible, Fluorescence Spectroscopies and Cyclic Voltammetry," *Journal of Photochemistry and Photobiology B: Biology* 124 (2013): 1–19.
41. F. Perveen, R. Qureshi, F. L. Ansari, S. Kalsoom, and S. Ahmed, "Investigations of Drug–DNA Interactions Using Molecular Docking, Cyclic Voltammetry and UV–Vis Spectroscopy," *Journal of Molecular Structure* 1004 (2011): 67–73.
42. H.-X. Zhou and X. Pang, "Electrostatic Interactions in Protein Structure, Folding, Binding, and Condensation," *Chemical Reviews* 118 (2018): 1691–1741.
43. S. Charak and R. Mehrotra, "Structural Investigation of Idarubicin–DNA Interaction: Spectroscopic and Molecular Docking Study," *Journal of Biological Macromolecules* 60 (2013): 213–218.
44. Y. Wang, D. T. Nguyen, G. Yang, et al., "A Modified MTS Proliferation Assay for Suspended Cells to Avoid the Interference by Hydralazine and β -Mercaptoethanol," *Assay and Drug Development Technologies* 19 (2021): 184–190.
45. E. Guenin, D. Ledoux, O. Oudar, M. Lecouvey, and M. Kraemer, "Structure-Activity Relationships of a New Class of Aromatic Bisphosphonates That Inhibit Tumor Cell Proliferation In Vitro," *Anticancer Research* 25 (2005): 1139–1145.
46. G. Dong, Y. Jiang, F. Zhang, F. Zhu, J. Liu, and Z. Xu, "Recent Updates on 1,2,3-, 1,2,4-, and 1,3,5-Triazine Hybrids (2017–Present): The Anticancer Activity, Structure–Activity Relationships, and Mechanisms of Action," *Archiv der Pharmazie* 356 (2023): 2200479.
47. X.-Y. Meng, H.-X. Zhang, M. Mezei, and M. Cui, "Molecular Docking: A Powerful Approach for Structure-Based Drug Discovery," *Current Computer-Aided Drug Design* 7 (2011): 146–157.
48. G. M. Morris, R. Huey, W. Lindstrom, et al., "AutoDock4 and AutoDockTools4: Automated Docking With Selective Receptor Flexibility," *Journal of Computational Chemistry* 16 (2009): 2785–2791.
49. J. Gillson, Y. Ramaswamy, G. Singh, et al., "Small Molecule KRAS Inhibitors: The Future for Targeted Pancreatic Cancer Therapy?," *Cancers* 12 (2020): 1341.
50. G. Zimmermann, B. Papke, S. Ismail, et al., "Small Molecule Inhibition of the KRAS–PDE δ Interaction Impairs Oncogenic KRAS Signalling," *Nature* 497 (2013): 638–642.
51. J. Luo, "KRAS Mutation in Pancreatic Cancer," *Seminars in Oncology* 48 (2021): 10–18.
52. P. Martín-Gago, E. K. Fansa, A. Wittinghofer, and H. Waldmann, "Structure-Based Development of PDE δ Inhibitors," *Biological Chemistry* 398 (2017): 535–545.
53. H. Zhong, Y. J. Zhang, and X. B. Shan, "Exploring Binding Modes of the Selected Inhibitors to Phosphodiesterase Delta by All-Atom Molecular Dynamics Simulations and Free Energy Calculations," *Journal of Biomolecular Structure & Dynamics* 37 (2019): 2415–2429.
54. G. Zimmermann, "Design, Synthesis and Biophysical Evaluation of Small Molecules Targeting the K-Ras-PDE δ Interaction," (diss., Durtmond Technical University, 2014).
55. H. A. Benesi and J. H. Hildebrand, "A Spectrophotometric Investigation of the Interaction of Iodine With Aromatic Hydrocarbons," *Journal of the American Chemical Society* 71 (1994): 2703–2707.
56. E. F. Pettersen, T. D. Goddard, C. C. Huang, et al., "UCSF Chimera—A Visualization System for Exploratory Research and Analysis," *Journal of Computational Chemistry* 13 (2004): 1605–1612.
57. BIOVIA, "Discovery Studio Modeling Environment," (Dassault Systeme, 2020).

Supporting Information

Additional supporting information can be found online in the Supporting Information section.

Supporting File 1: cbdv70296-sup-0001-SupMat.pdf